Neurobiology of Learning and Memory 164 (2019) 107042

Contents lists available at ScienceDirect

Neurobiology of Learning and Memory

journal homepage: www.elsevier.com/locate/ynlme

Reduced perineuronal net expression in *Fmr1* KO mice auditory cortex and amygdala is linked to impaired fear-associated memory

Sarah M. Reinhard[a], Maham Rais[b], Sonia Afroz[b], Yasmien Hanania[b], Kasim Pendi[b], Katherine Espinoza[a,b], Robert Rosenthal[a], Devin K. Binder[b,c], Iryna M. Ethell[b,c,*], Khaleel A. Razak[a,c,*]

[a] Psychology Department and Psychology Graduate Program, University of California, Riverside, CA 92521, USA
[b] Division of Biomedical Sciences, School of Medicine, University of California, Riverside, CA 92521, USA
[c] Neuroscience Graduate Program, University of California, Riverside, CA 92521, USA

ARTICLE INFO

Keywords:
Fragile X syndrome
Learning deficits
Fear conditioning
Perineuronal nets
Parvalbumin
Auditory cortex

ABSTRACT

Fragile X Syndrome (FXS) is a leading cause of heritable intellectual disability and autism. Humans with FXS show anxiety, sensory hypersensitivity and impaired learning. The mechanisms of learning impairments can be studied in the mouse model of FXS, the *Fmr1* KO mouse, using tone-associated fear memory paradigms. Our previous study reported impaired development of parvalbumin (PV) positive interneurons and perineuronal nets (PNN) in the auditory cortex of *Fmr1* KO mice. A recent study suggested PNN dynamics in the auditory cortex following tone-shock association is necessary for fear expression. Together these data suggest that abnormal PNN regulation may underlie tone-fear association learning deficits in *Fmr1* KO mice. We tested this hypothesis by quantifying PV and PNN expression in the amygdala, hippocampus and auditory cortex of *Fmr1* KO mice following fear conditioning. We found impaired tone-associated memory formation in *Fmr1* KO mice. This was paralleled by impaired learning-associated regulation of PNNs in the superficial layers of auditory cortex in *Fmr1* KO mice. PV cell density decreased in the auditory cortex in response to fear conditioning in both WT and *Fmr1* KO mice. Learning-induced increase of PV expression in the CA3 hippocampus was only observed in WT mice. We also found reduced PNN density in the amygdala and auditory cortex of *Fmr1* KO mice in all conditions, as well as reduced PNN intensity in CA2 hippocampus. There was a positive correlation between tone-associated memory and PNN density in the amygdala and auditory cortex, consistent with a tone-association deficit. Altogether our studies suggest a link between impaired PV and PNN regulation within specific regions of the fear conditioning circuit and impaired tone memory formation in *Fmr1* KO mice.

1. Introduction

Inappropriate activation of fear-associative circuits can become an impediment to daily function, causing arousal, anxiety and aversion to stimuli that are not threatening. Behavioral tools that include fear conditioning have been useful in studying anxiety disorders. Indeed people with anxiety show heightened fear responses (Duits et al., 2015; Lissek et al., 2005) and regions of the central nervous system that are known to be active during fear conditioning (Andreatta et al., 2015; LaBar, Gatenby, Gore, LeDoux, & Phelps, 1998) show abnormal activation (reviewed in Shin & Liberzon, 2010). Many neurodevelopmental disorders share heightened anxiety as a core feature, including Fragile X Syndrome (FXS). FXS is the leading cause of heritable intellectual disability and one of the most prevalent monogenic causes of autism (reviewed in Hagerman & Hagerman, 2002; Santoro, Bray, & Warren, 2012; Yoo, 2015). It is caused by an increase in the number of CGG repeats that lead to hypermethylation of *fragile X mental retardation gene-1* (*Fmr1*) and a reduction of the protein product, FMRP. Symptoms of FXS include intellectual disabilities, attention deficits (Cornish, Munir, & Cross, 2001), stereotyped behaviors, sensory processing deficits (Miller et al., 1999) and increased anxiety, which can manifest as aggression, social withdrawal, and gaze aversion (Sullivan, Hooper, & Hatton, 2007).

One commonly studied mouse model of FXS is generated by deletion of the *Fmr1* gene (*Fmr1* KO mouse; Bakker & Oostra, 2003; Kooy et al.,

Abbreviations: AC, auditory cortex; BLA, basolateral amygdala; FrC, fear conditioning; FXS, fragile X syndrome; LA, lateral amygdala; MMP-9, matrix metalloproteinase-9; Nv, naïve conditioned; PNN, perineuronal nets; PV, parvalbumin

* Corresponding authors at: Division of Biomedical Sciences, School of Medicine, University of California, Riverside, CA 92521, USA (I.M. Ethell). Psychology Department and Psychology Graduate Program, University of California, Riverside, CA 92521, USA (K.A. Razak).

E-mail addresses: iryna.ethell@medsch.ucr.edu (I.M. Ethell), Khaleel@ucr.edu (K.A. Razak).

https://doi.org/10.1016/j.nlm.2019.107042
Received 7 February 2019; Received in revised form 20 June 2019; Accepted 10 July 2019
Available online 18 July 2019
1074-7427/

1996; Paradee et al., 1999) and recapitulates many phenotypes of FXS (Castrén, Pääkkönen, Tarkka, Ryynänen, & Partanen, 2003; Dziembowska et al., 2013; Lovelace et al., 2016; Sidhu, Dansie, Hickmott, Ethell, & Ethell, 2014). While multiple groups have shown altered fear memory in *Fmr1* KO mice, the mechanisms underlying the deficits remain unclear (de Diego-Otero et al., 2009; Dobkin et al., 2000; Eadie, Cushman, Kannangara, Fanselow, & Christie, 2012; Olmos-Serrano, Corbin, & Burns, 2011; Paradee et al., 1999; Romero-Zerbo et al., 2009).

The regions involved in fear conditioning have been well characterized and include the amygdala (Phillips & LeDoux, 1992; Quirk, Armony, & LeDoux, 1997), hippocampus (Daumas, 2005; Esclassan, Coutureau, Di Scala, & Marchand, 2009; Roy et al., 2017) and the sensory cortices, including the auditory cortex (Antunes & Moita, 2010; Froemke, Merzenich, & Schreiner, 2007; Letzkus et al., 2011). The cellular mechanisms underlying fear conditioning are also beginning to be understood. Inhibitory neurons across these regions, including parvalbumin (PV) expressing cells, play a pivotal role in shaping the memory engram. Perturbing the function of PV cells can alter the formation of a fear memory (Morrison et al., 2016; Ognjanovski et al., 2017). Conversely, increasing PV cell activity can increase the persistence of a fear memory (Çalışkan et al., 2016). Similarly, perineuronal nets (PNN), which are specialized assemblies of extracellular matrix, play an important role in fear-conditioning circuits. In particular, PNNs ensheath a large percentage of PV cells (Dityatev et al., 2007; Lee, Leamey, & Sawatari, 2012; McRae, Rocco, Kelly, Brumberg, & Matthews, 2007; Ueno et al., 2018) and shape the firing properties of these cells (Balmer, 2016; Dityatev et al., 2007; Favuzzi et al., 2017). PNNs act as a "brake" on formation of new synaptic contacts (Carstens, Phillips, Pozzo-Miller, Weinberg, & Dudek, 2016; Gogolla, Caroni, Lüthi, & Herry, 2009) or can stabilize existing synapses. While reorganization of PNNs is necessary for new long-term memory formation (Happel et al., 2014; Xue et al., 2014) and/or consolidation after fear conditioning (Banerjee et al., 2017; Hylin, Orsi, Moore, & Dash, 2013), PNNs also preserve fear-associated memories over time (Gogolla et al., 2009) and disruption of PNNs impairs fear memory acquisition (Banerjee et al., 2017; Hylin et al., 2013).

While the role of PNNs in developmental plasticity has been well described (Takesian & Hensch, 2013), an emerging literature suggests that even in adult brains PNNs are highly and rapidly responsive to learning related modifications (Beurdeley et al., 2012) including addiction and environmental enrichment (Slaker et al., 2015; Slaker, Barnes, Sorg, & Grimm, 2016; Slaker, Blacktop, & Sorg, 2016; Slaker, Harkness, & Sorg, 2016). A recent study showed that changes in PNN density in the auditory cortex is necessary for tone-associated fear learning (Banerjee et al., 2017). We have shown deficits in both PV and PNN in the developing auditory cortex of *Fmr1* KO mice (Wen, Afroz, et al., 2018), consistent with observations that altered PNN density and function may underpin multiple brain disorders (reviewed in Wen, Binder, Ethell, & Razak, 2018). Taken together, these studies suggest that abnormal PNN dynamics in the auditory cortex and potentially within other regions of the fear learning circuit in *Fmr1* KO mice may cause impaired fear conditioning observed in this mouse model. We tested this hypothesis by first confirming a tone-associated fear learning deficit in *Fmr1* KO mice compared to WT mice and then examining the density, intensity and changes in PV and PNN cells in the *Fmr1* KO mouse auditory cortex, amygdala and hippocampus in response to fear conditioning.

2. Methods

2.1. Mice

Breeding pairs of FVB.129P2-Pde6b^{+}Tyr$^{c\text{-}ch}$ Fmr1^{tm1Cgr}/J (Jax 004624; *Fmr1* KO) and their congenic controls FVB.129P2-Pde6b^{+}Tyr$^{c\text{-}ch}$/AntJ mice (Jax 002848; WT) were obtained from the Jackson Laboratory and housed in an accredited vivarium on a 12-hlight/dark cycle. Food and water were provided *ad libitum* and confirmation of genotypes was conducted using PCR analysis of genomic DNA isolated from tail clippings. University of California, Riverside's Institutional Animal Care and Use Committee approved all procedures used. Experiments were conducted in accordance with NIH *Guide for the Care and Use of Laboratory Animals*. The total number of mice used for behavior tests was: WT Naïve = 24, WT Fear Conditioned = 32; *Fmr1* KO Naïve = 22, *Fmr1* KO Fear Conditioned = 26. From these, 10–11 mice per group were used for immunohistochemistry. Naïve conditioned mice (Nv) underwent all handling/habituation/training and recall but without the shock (tone was still played). Fear conditioned mice (FrC) underwent all procedures including the tone/shock pairing during training. An additional 7 WT mice and 6 *Fmr1* KO mice, which we reference as control mice (C), were those raised in the vivarium and tested without any exposure to the fear conditioning arena. All mice used were 2–4 month old males.

2.2. Fear conditioning

Mice were handled in the training room for 5 days prior to training, with ~2 min of handling per day for each mouse. Mice were acclimated to the training room for at least 30 min daily before any testing/handling took place.

Day 1: Mice were habituated to the training and recall contexts (context A and context B) for 10 min each. Context A is the training context, where mice receive a shock (unconditioned stimulus; US) paired with a tone (conditioned stimulus; CS), and are retested 24 h later for context recall. Context A is a square arena with metal walls and metal grid bars on the floors; it has white lighting and is scented with Quatricide. Context B is where mice undergo tone recall; this is a square arena with checker-patterned walls, inside of which is placed a circular glass arena that has bedding on the floors; it has yellow lighting and is scented with Windex. The combination of different tactile, visual and olfactory information was to ensure that mice do not generalize from training in context A to tone recall testing in context B. The arena was cleaned after each mouse, using: (context A) 70% ethanol, Quatricide, and DiI water followed by a further spray of Quatricide; or (context B) 70% ethanol, Windex and DiI water, followed by a further spray of Windex.

Day 2: Training in context A occurred 24 h after habituation. Mice had a period of 3 min of silence after being placed in context A, followed by 5 CS-US pairings (30 s tone, 9 kHz, 78–80 dB; co-terminating with a scrambled footshock, 2 s, 0.6 mA). The interval between each of the 5 CS-US pairing was pseudo-random (60–120 s) to avoid an association with the delay interval between tones.

Day 3: 24 h after fear conditioning, mice were tested for their recall of the context- and tone- associated fear memories. This included, in context B, a baseline measurement of normal activity levels and then tone recall (baseline: 3 min of silence; tone recall: 3 min with tone), and in context A, context recall as well as context + tone recall (context recall: 3 min of silence; context + tone: 3 min with tone). The order that recall was tested (context then tone recall vs. tone then context recall) was counterbalanced between mice, with at least 1 h between each recall test. Mice used for further tissue processing had 3 h and 30 min between the first and second contexts and were perfused 30 min after the last recall. Modification of PNNs can occur within 4 h of a training event, so this timing was planned to control for any modification of the circuit after re-exposure to fear-associated cues without the shock reinforcement (Banerjee et al., 2017). Two control groups were included, (1) control mice taken directly from their home cage in the vivarium and immediately perfused; (2) naïve mice that underwent an identical protocol as conditioned mice except without the footshock at the end of the tone. The experimenter was blinded to the genotype of mice throughout training, and blind to the condition (Nv or FrC) except on training day. Mice were trained and tested in a pseudo random order when possible to avoid order effects.

Statistics. Freezing was measured using Freezeframe software (Colbourn Instruments, Holliston, MA, USA), with a threshold of 1 s for determining "freezing" behavior. Videos were further manually checked to determine whether the software measurement of "freezing" behavior was consistent with observed freezing behavior. Three-way or two-way ANOVA was used (repeated measures for training and recall) as appropriate with Bonferroni-corrected paired comparisons. The corrected p-value is reported for all paired comparisons (p-value * #comparisons). An unpaired *t*-test was used to compare freezing during habituation. Statistical analysis was performed using Graphpad Prism 6 or SPSS. Mean and SEM are reported as (M ± SEM). We report the r-effect size (*t*-test) or partial eta-squared (η^2) effect size (ANOVA) and the 95% CI for the effect sizes (methods in: Tellez, Garcia, & Corral-Verdugo, 2015).

2.3. Analysis of additional behaviors in fear conditioned mice

To further understand the behavioral response characteristics of *Fmr1* KO mice after fear conditioning, videos from a subset of mice were randomly selected and manually scored, using six categories of mouse behaviors which were based on studies of elevated plus maze (Table 1; Coimbra et al., 2017; Cruz, Frei, & Graeff, 1994; Rodgers & Johnson, 1995) and adapted for our purposes.

Videos were scored at 10 s intervals during: (1) baseline (context B; 3 min; silence), (2) tone recall (context B; 3 min; tone), (3) context recall (context A; 3 min; silence) and (4) context + tone recall (context A; 3 min; tone) using 9–11 mice per group (WT, *Fmr1* KO; N, FrC). At every interval, the recording was paused and the observer noted which behavior was in progress according to the parameters established (Table 1). The percentage of total observations was calculated (18 observations for each 3 min recall session) of a behavior and analyzed with a two-way RM ANOVA for each recall session separately.

2.4. Immunocytochemistry and image analysis

Naïve and FrC mice were sacrificed 30 min after the last recall test with isoflurane and perfused transcardially with cold phosphate-buffered saline (PBS, 0.1 M) and 4% paraformaldehyde (PFA). Control mice were perfused immediately after removal from their home cages. Brains were removed and post-fixed for 2–4 h in 4% PFA. 100 μm coronal sections were obtained using a vibratome (Campden Instruments 5100 mz Ci). For each animal, 3–5 slices containing auditory cortex (from bregma: −2.03 mm to −2.53 mm), dorsal hippocampus (−1.91 mm to −2.53 mm) and amygdala (−1.91 mm to −2.15 mm; Allen Mouse Brain Atlas) were taken and processed for immunohistochemistry. Approximately the same rostral-caudal range of slices was used for each animal. To determine whether the order of recall testing leads to differential PV and PNN modifications the order of recall testing was treated as two separate experiments (context-tone *or* tone-context).

5–6 animals per condition (2 treatment (Nv, FrC) × 2 genotypes (WT, *Fmr1* KO)) were tested in each experiment (context-tone *or* tone-context). In order to control for differences in staining between rounds of IHC, one slice from each mouse within an experiment (20–22 mice, 1 slice each) was included in the 24-well plate, with additional 1–3 slices from control mice. Typically all slices were imaged within a week of staining. In this way, differences between conditions could not be due to differences in staining quality, tissue processing or imaging. This process was repeated until 3–5 slices per mouse were stained and imaged. Control mouse data were combined from both experiments and presented with figures in text. For staining, slices were post-fixed for an additional 2 h in 4% PFA and then washed (3×, 10 min) in 0.1 M PBS. Slices were then quenched with 50 mM ammonium chloride for 15 min and washed with PBS (3×, 10 min). Next, brain tissue was permeabilized with 0.1% triton-X in PBS. Afterwards non-specific staining was blocked with a 5% Normal Goat Serum (NGS) (Vector Laboratories) and 1% Bovine Serum Albumin (BSA) (Fisher Scientific) in 0.1 M PBS solution. Slices were incubated overnight with primary antibody rabbit-anti PV (1:1000; SWANT PV25) and Wisteria floribunda agglutinin (WFA) in a 1% NGS, 0.5% BSA, and 0.1% tween solution. WFA (1:500; Vector Laboratories; Green Florescein Wisteria Floribunda Lectin FL 1351) is a lectin that binds to chondroitin sulfate proteoglycan glycosaminoglycan side chains, which make up PNN (Pizzorusso et al., 2002). After overnight incubation with primary antibody and WFA at 4 °C, slices were washed in 0.5% tween (3×, 10 min) and incubated at room temperature with secondary antibodies in 0.1 M PBS for 1 h. Secondary antibodies used were Alexa donkey-anti-rabbit 594 (1:500; Invitrogen). Finally, slices were washed with 0.5% tween (2×, 10 min) and 0.1 M PBS (1×, 10 min), mounted in Vectashield with DAPI (Vector Labs), and cover-slipped with Cytoseal (ThermoScientific). It is important to note that the PNNs analyzed in this study are only WFA-positive PNNs. Instead of using 'WFA-stained PNN', we use 'PNN' for brevity.

Slices were imaged using Leica SP5 confocal microscope (10× objective). Microscope settings were consistent across all images for intensity comparisons. Imaged Z-stacks covering 10 μm (1 μm step size) were selected from each slice and 3-D projections were created using ImageJ. We collected optical images 1–10 μm from the surface of the slice due to antibody penetration considerations deeper into the section. ImageJ was used to count number of PNN positive cells, number of PV positive cells, and number of cells co-localized with PNN and PV by a blinded observer.

Slaker, Barnes, et al. (2016), Slaker, Blacktop, et al. (2016) and Slaker, Harkness, et al. (2016) introduced a standardized methodology for analyzing intensity and cell counts of PNNs called PIPSQUEAK. We performed PIPSQUEAK analysis in addition to the manual counting using ImageJ as an independent validation of the differences between genotypes. For intensity analysis, 10 images in the Z-stack (1.194 pixels/μm) were compiled into a single image using ImageJ macro plug-in PIPSQUEAK (https://labs.wsu.edu/sorg/research-resources/), scaled, and converted into 32-bit, grayscale, tiff files. PIPSQUEAK was run in "semi-automatic mode" to select ROIs to identify individual PV cells and PNNs, which were then verified by a trained experimenter who was blinded to the experimental conditions. The plug-in compiles this analysis to identify single- (Slaker, Barnes, et al., 2016; Slaker, Blacktop, et al., 2016; Slaker, Harkness, et al., 2016), double-, and triple-labeled neurons (Harkness et al., 2018; https://ai.RewireNeuro.com). Control group mean cell intensities were used to calculate

Table 1
Definition of mouse behaviors (Coimbra et al., 2017; Cruz et al., 1994; Rodgers & Johnson, 1995).

Behavior	Definition
Immobility	Complete stillness without head and body movement
Scanning	Head orienting, sniffing, air sampling, without body movement
Stretch attend posture (SAP)	Forward elongation of the body followed by retreat to original posture or pivoting within a circle
Self-grooming	Species-typical sequence that begins with grooming of the snout, progressing to the ears and ending with whole body
Digging	Using the paws to dig through bedding
Rearing	Bipedal posture is supported with the hind paws
In motion	Any action that incorporates both the front and hind paws and allows for full body movement

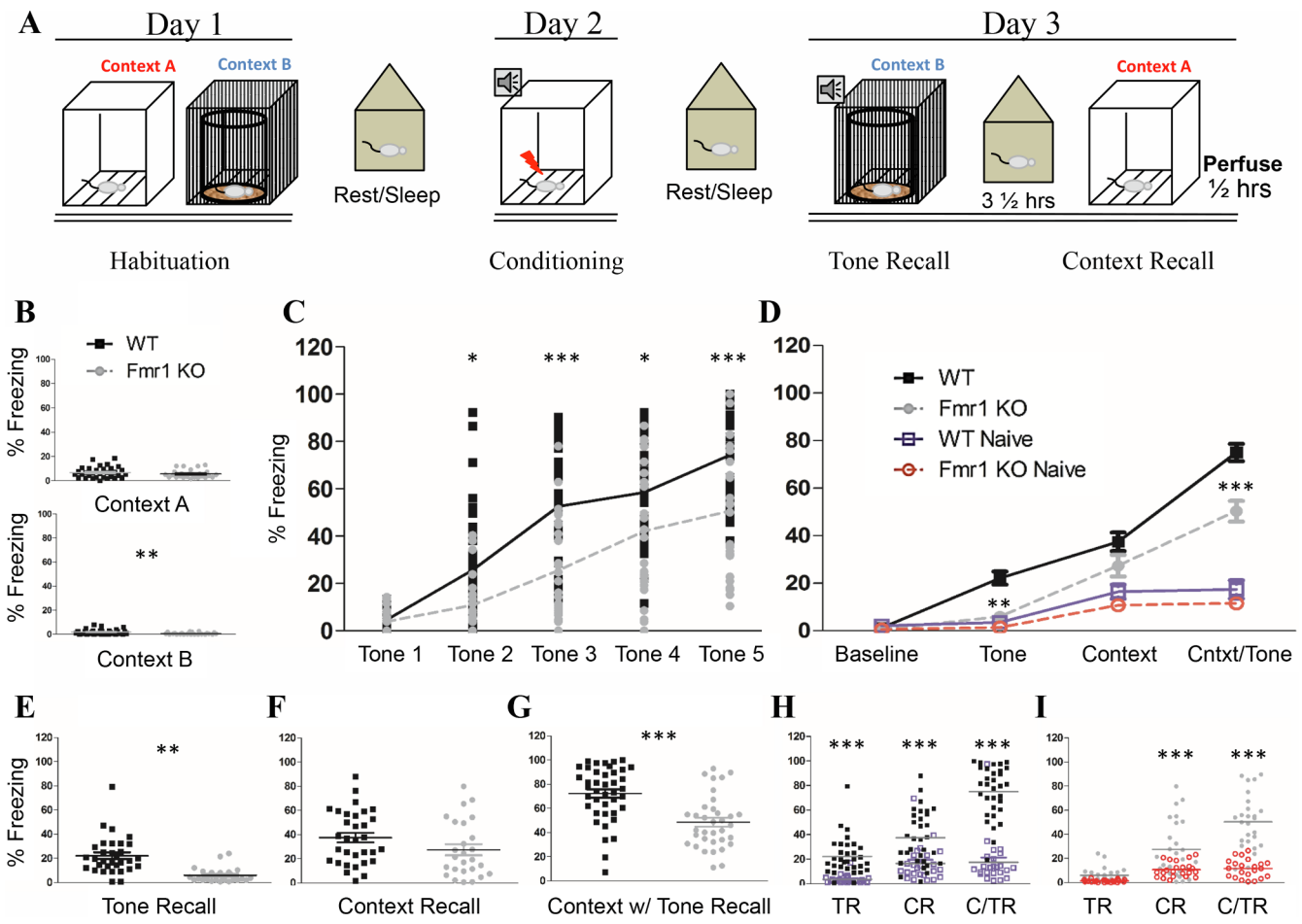

Fig. 1. Impaired tone recall in *Fmr1* KO mice after fear conditioning. (A) Schematic of training protocol: On day 1, mice were habituated to Context A and Context B for 10 min each. 24 h later mice were trained with 5 tone-shock parings in Context A and returned to their home cage. Recall of the tone and context memories were tested 24 h later with 3½ h between tests. 30 min after the final recall session brain tissue was harvested. (B) Habituation: All animals had low levels of freezing during habituation. (C) During training both genotypes increased their freezing significantly across the training session from Tone 1 to Tone 5; however FrC *Fmr1* KO mice consistently froze at a lower level than FrC WT mice. (D) 24-h Recall: *Fmr1* KO mice had impaired freezing during tone recall and contextual + tone. (Individual data for each test is shown in E, F and G). (H) FrC WT mice froze more than Nv WT on all three recall tests; (I) but FrC *Fmr1* KO mice increased freezing to context and context + tone recall only. Asterisks indicate results from *t*-test (B) or paired comparison from a two-way (C) or three-way (D–I) RM ANOVA. (*, **, ***/p = 0.05, 0.01, 0.001). N: WT Nv = 24; WT FrC = 32; *Fmr1* KO Nv = 22; *Fmr1* KO FrC 26.

normalized intensities for each stain. Distributions of normalized intensities were then compared between experimental groups, to assess differences in intensities between WT and *Fmr1* KO mice under all 3 conditions (control, naïve and fear conditioned).

In hippocampus and auditory cortex a fixed area was used for analysis across all images (see photomicrographs of Figs. 1–4). For CA1, a 381 × 1000 μm^2 box was used for analysis, aligned with the superficial edge of dentate gyrus granule cell layer. In CA2 a triangle radiating at a 45° angle from the superficial edge of dentate gyrus (dimensions: 768 × 538 × 1015 μm) was used for analysis. This same triangle was used for intensity measurements in CA2, where the mean intensity was measured inside the triangle with background subtracted (mean intensity within a 5 μm × 5 μm box). CA3 analysis was within a freehand polygon shape (357,617 μm^2 area) beginning from the inferior edge of dentate gyrus taking care that CA2 and CA3 area did not overlap. For the dentate gyrus, a 520 × 1537 μm^2 box was used for analysis and cells from the tail end of CA3 within the box were excluded. A box of 500 μm width and spanning from pia to white matter was used to analyze auditory cortex (AC). The layer specific counts in AC were determined based on a previously published study (Anderson, Christianson, & Linden, 2009), where 50% of the length between pia and white matter was used as the boundary between deep and superficial layers. A fixed area of analysis could not be used in the amygdala because the size of the structure varies from rostral to caudal slices. Therefore a freehand tool was used to select amygdala. Lateral and basolateral amygdala were determined from the Allen Mouse Brain Atlas, visible landmarks and PV/PNN expression patterns. Two-way ANOVA was used to compare between genotype and condition for each brain region. Bonferroni correction was used for post-hoc analysis. When the initial ANOVA indicated an overall effect of conditioning, because there were 3 conditions (C, Nv and FrC) it could not be determined which groups were different using our statistical package. Therefore, additional two-way ANOVAs were used to determine if the difference was between Nv and C, Nv and FrC *or* C and FrC mice. This was necessary for understanding the effects of fear conditioning independent of naïve conditioning, and will be noted as "2-Cond Test" in text. These values were only reported as significant if they met the Bonferroni corrected significance value of (0.05/3 tests) p = 0.0166.

2.5. Correlation of freezing levels and cell counts

To better understand the relationship between the cell counts and the freezing behavior of mice, correlations were calculated between the freezing levels of each mouse (for context, tone and context + tone recall) and the observed density of PV cells, PNN cells and co-localized PV/PNN in different brain regions examined. All animals used for tissue

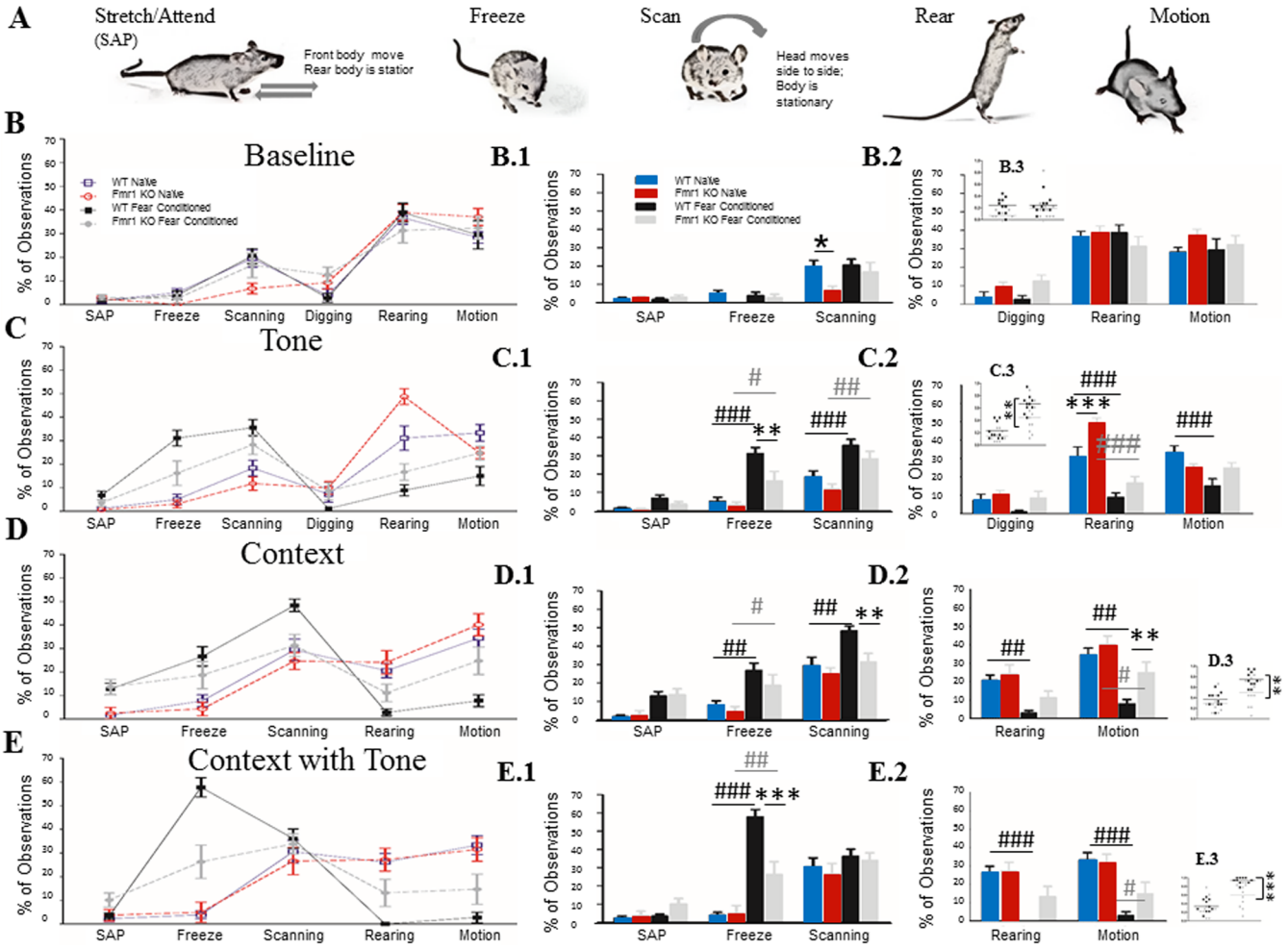

Fig. 2. Manual analysis of characteristic mouse behaviors, confirms lower freezing and less alteration of baseline behaviors in *Fmr1* KO mice. (A) Characteristic mouse behaviors used for scoring recall tests. (B) Baseline showed no overall difference in observed behaviors between WT and *Fmr1* KO mice, either with "anxious-like" (B.1) or "non-anxious-like" (B.2) behaviors. C) During Tone recall, *Fmr1* KO mice froze less than WT mice consistent with the computer-analyzed data. Both genotypes increased freezing after conditioning compared to naïve control mice (C.1); both genotypes also increased their scanning after fear conditioning and decreased their rearing after fear conditioning (C.2). Only WT mice decreased their bouts of motion. D) During context recall both WT and *Fmr1* KO mice increased their freezing after training, and decreased their motion; however only WT mice increased their scanning (D.1) and showed reduced rearing (D.2). Finally, during context + tone recall, both WT and *Fmr1* KO increased their freezing after training, but *Fmr1* KOs froze significantly less than WTs (E.1). WT mice decreased their rearing and motion (E.2), whereas *Fmr1* KO mice decreased their motion but not rearing. (C.3/D.3/E.3) When both scanning and freezing are combined we see that *Fmr1* KO mice show a deficit even in contextual recall. Within genotype effect of conditioning #, ##, ###; genotype effect *, **, *** (p = 0.05, 0.01, 0.001). N: WT Naïve = 10, WT FrC = 10, *Fmr1* KO Naïve = 9, *Fmr1* KO FrC = 11. All asterisks reflect paired comparisons from a three-way RM ANOVA (column 1 and 2) or two-way ANOVA (column 3).

processing were included in this analysis. WT and *Fmr1* KO mice were first combined to assess overall correlation among all mice. Additionally, a regression curve and R-value for WT and *Fmr1* KO groups was calculated separately, and the R-values of each genotype were compared.

To test the null hypothesis that R-values are from the same population the following was used, where r is the R-value taken from the regression analysis, Zr is a Fisher's Z transformation of r:

(1) Convert r values to Zr: $Zr = (0.5)\ln[\frac{1+r}{1-r}]$

(2) Compute test statistic: $z = \frac{Zr1 - Zr2}{\sqrt{\sqrt{\frac{1}{n1-3} + \frac{1}{n2-3}}}}$

3. Results

3.1. Mouse behavior

3.1.1. Tone fear memory is impaired in Fmr1 KO mice

Mice were first habituated to each context. During habituation, WT and *Fmr1* KO mice showed no difference in baseline activity levels (overall low freezing) in context A ($p = 0.25$). There was a difference in context B ($p = 0.0046$) driven by almost no freezing in the majority of *Fmr1* KO mice (Table 2; Fig. 1B). During training, both genotypes showed an increase in freezing from the first CS-US pairing to the last CS-US pairing, indicating both WT and *Fmr1* KO mice responded with increased freezing to the CS-US pairing (effect of training: $p < 0.0001$). However, *Fmr1* KO mice did not freeze to the level of WT mice (effect of genotype: $p < 0.0001$; Fig. 1C). Though *Fmr1* KO mice freeze less than the WT, when compared to their conspecific naïve *Fmr1* KO mice they did significantly increase their freezing levels by tone 4 and 5, indicating they did respond to the training (tone 4: $p < 0.00005$; tone 5: $p < 0.00005$; effect of training: $p < 0.0001$; effect of conditioning: $p < 0.0001$).

Mice were tested 24 h later for tone recall in context B (tone recall), context A recall (context recall) and context A recall with the tone (context + tone), including a baseline freezing measurement. A repeated measures ANOVA revealed significant differences in freezing levels between the different recall tests (within subjects: $p < 0.0001$)

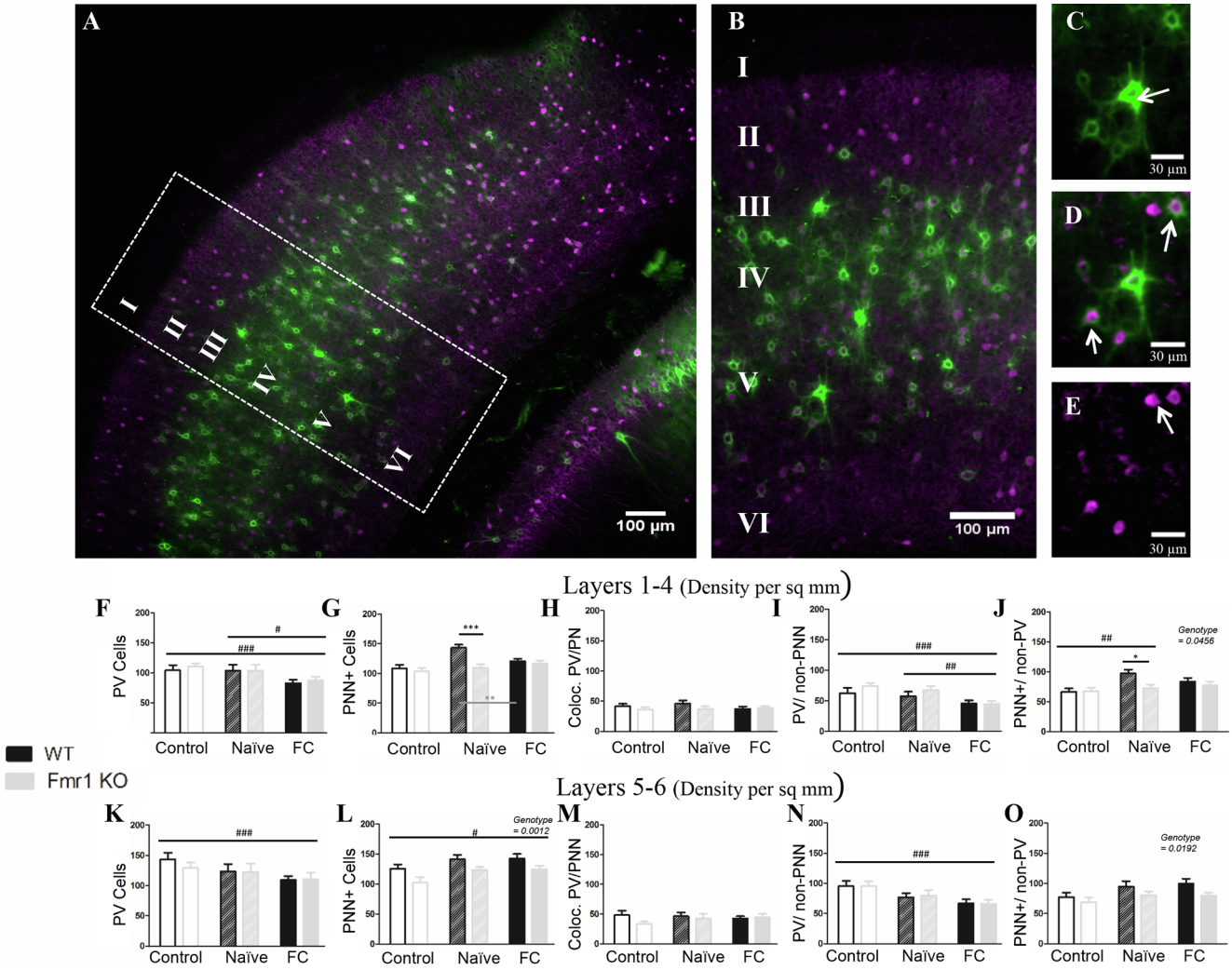

Fig. 3. Fear conditioning causes reduced PV density across genotypes in auditory cortex, and dysregulation of PNNs in auditory cortex of *Fmr1* KO mice. (A) Example image of WT naïve auditory cortex, with cropped image used for analysis (B). The far right panels identify examples of PNN surrounding non-PV cells (C; arrow), PV cells without PNN (E; arrow) and co-localized PV/PNN cells (D; arrow). F) Fear conditioning caused a decrease in PV density in both superficial (K) and deep layers, specifically in PV cells that were not surrounded by PNN (I; N). There was no genotype difference in PV cell density. L) There were overall fewer PNN cells in *Fmr1* KO auditory cortex (deep layers), which were surrounding non-PV cells (O), but no difference was seen in PNNs which surround PV cells (H; M). In superficial layers WT mice up-regulate PNNs after naïve conditioning, and down-regulate them after fear conditioning, while *Fmr1* KO mice show no change (G). Conditioning effect #, ##, ###; paired comparison *, **, *** (p = 0.05, 0.01, 0.001). N per group: WT Nv = 5; WT FrC = 5; WT C = 3, *Fmr1* KO Nv = 6, *Fmr1* KO FrC = 6, *Fmr1* KO C = 5. Image # per group: WT Nv = 19, WT FrC = 18, WT C = 15, *Fmr1* KO Nv = 18, *Fmr1* KO FrC = 18, *Fmr1* KO C = 18.

as well as between genotypes ($p < 0.0001$) reflecting overall lower levels of freezing in *Fmr1* KO mice across all tests. There was also an effect of the training condition ($p < 0.0001$) indicating that FrC mice froze at higher levels than Nv mice (Table 2, Fig. 1D).

Paired comparison revealed that baseline freezing (context B without a tone; Fig. 1D) was not different between FrC WT and *Fmr1* KO mice ($p = 0.88$). During recall testing, *Fmr1* KO mice showed a deficit in tone recall ($p < 0.0019$; Fig. 1E) and a deficit in context + tone recall ($p = 0.00004$; Fig. 1G), but with no significant difference when context recall was tested ($p = 0.10$; Fig. 1F; Table 3).

The similar levels of activity and/or freezing during baseline measurement suggest similar locomotor activity in both genotypes. However, many studies have found increased locomotor activity in *Fmr1* KO mice (de Diego-Otero et al., 2009; Oddi et al., 2015; Olmos-Serrano et al., 2011; Thomas et al., 2011) and it remains possible that the consistently low freezing observed in *Fmr1* KO mice may be partially due to hyperactivity that affects automated freezing measurements. To clarify whether this is the case, each FrC genotype was compared to its own Nv controls on the 3 recall tests. If increased freezing is observed in FrC mice compared to Nv mice, this is evidence of formation of a fear-associated memory, independent of genotype differences in activity. WT FrC mice increased their freezing significantly compared to WT Nv mice on tests of tone recall ($p = 0.00063$), context recall ($p = 0.00012$) and context + tone ($p < 0.00003$; Fig. 1H; Table 3).

FrC *Fmr1* KO mice were not different from Nv *Fmr1* KO mice on the tone recall test ($p = 0.83$) but displayed higher freezing during context recall ($p = 0.00072$) and in the context + tone recall ($p < 0.00003$). Baseline freezing was not different between Nv and FrC mice in either genotype (data not shown). This confirms that reduced freezing during tone recall in *Fmr1* KO mice is independent of possible genotype specific locomotion/activity differences and reflects a deficit in tone-associated fear memory.

Finally, to eliminate the possibility that deficits in fear memory recall were due to impaired training in the *Fmr1* KO mice, we re-ran our analysis to exclude all *Fmr1* KO mice that did not train at least to WT levels by tone 5 of the training session. The lowest level of freezing among WT mice during tone 5 was 38%. Therefore, any *Fmr1* KO mice

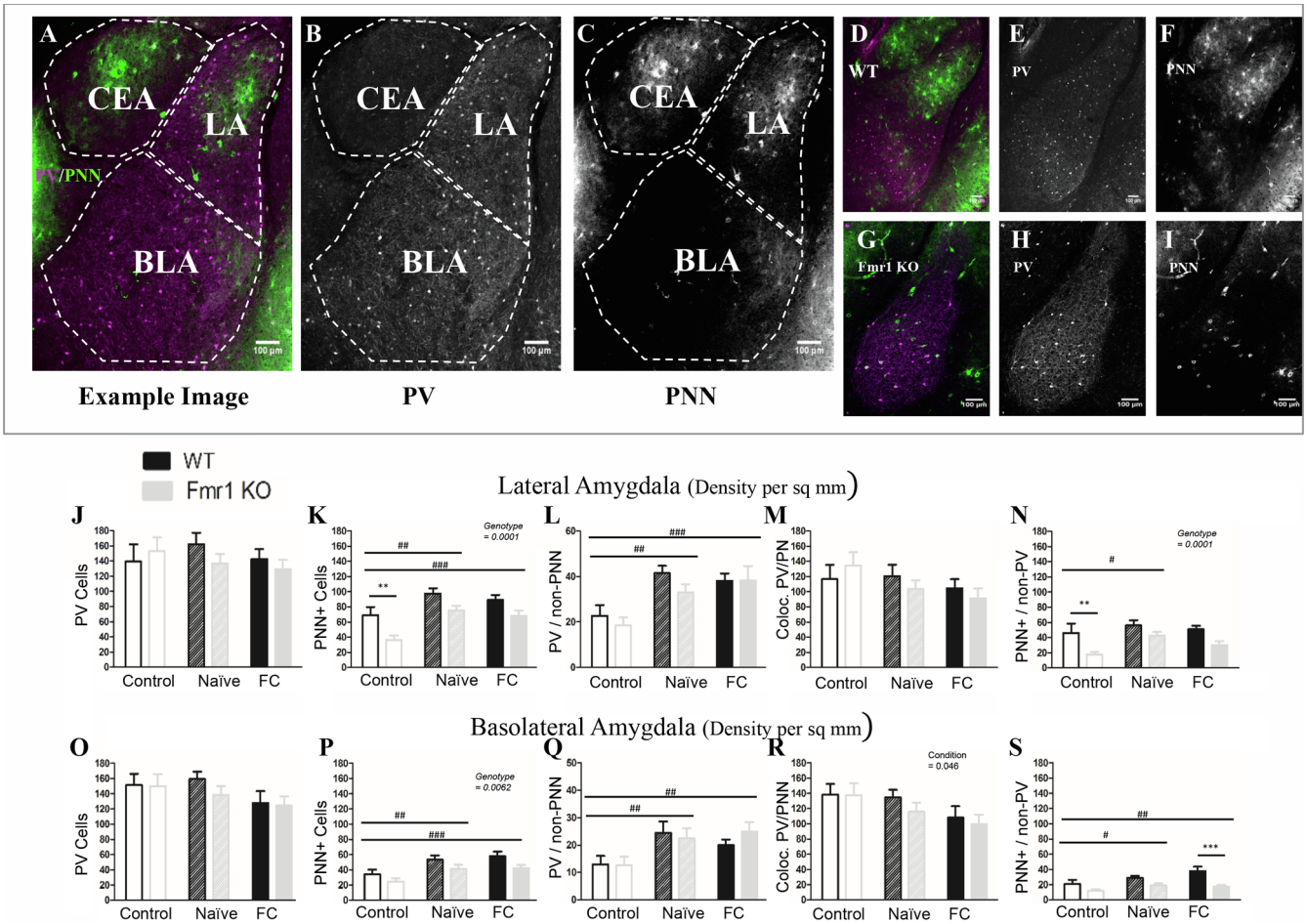

Fig. 4. *Fmr1* KO mice have less PNN in the amygdala than WT mice, but can still upregulate PNNs after conditioning. (A) Example image from a coronal section containing amygdala nuclei, including the lateral nucleus (LA), the basolateral nucleus (BLA) and the central nucleus (CEA). CEA was not identifiable in all slices and therefore was not counted. Area of each nucleus is determined using visible anatomic structures, gradation in cellular staining and the mouse Allan brain atlas. PV (B) and PNN (C) are shown to the right. (D) Example image of a WT naïve slice and an (G) *Fmr1* KO naïve slice, with PV (E; H) and PNN (F; I) to the right. Overall there are fewer PNNs in *Fmr1* KO mice than WT in both LA (K) and BLA (P), specifically fewer PNNs surrounding non-PV cells (N; S). This genotype difference is not affected by conditioning. Both naïve and fear conditioned mice show an increase in PNNs across genotypes. J; O) While there was no difference in overall PV cell number either due to conditioning or to genotype, it seems that both the naïve exposure to the training protocol as well as full conditioning cause an increase in the number of PV cells that are surrounded by PNN (L; Q) probably due to increased overall PNN. At the same time there was a reduction in PV cells not surrounded with PNN after fear conditioning in the BLA (R) but not in the LA (M). Conditioning effect #, ##, ###; paired comparison *, **, *** (p = 0.05, 0.01, 0.001). N per group: WT Nv = 5; WT FrC = 6; WT C = 3, *Fmr1* KO Nv = 6, *Fmr1* KO FrC = 6, *Fmr1* KO C = 4. Image # per group: WT Nv = 17, WT FrC = 17, WT C = 13, *Fmr1* KO Nv = 17, *Fmr1* KO FrC = 17, *Fmr1* KO C = 17.

that froze less than 38% during tone 5 were excluded for this analysis. Analysis showed that 14 mice froze at least to 38% by tone 5, out of the 24 total *Fmr1* KO mice (Sup. Fig 1A). This analysis demonstrated that both WT and *Fmr1* KO groups froze to comparable levels by tones 4 and 5 (tone 4: p = 0.49; tone 5: p = 0.69). Nevertheless, 24 h after training, *Fmr1* KO mice froze significantly less during the tone recall (p = 0.037) and context + tone (p = 0.00018) recall tests (Sup. Fig. 1B; Table 4) but not during context recall (p = 0.28). Taken together, these analyses confirm deficits in tone and context + tone recall in *Fmr1* KO mice independent of training differences between genotypes.

3.1.2. Fmr1 KO mice show similar "exploratory" and "fear" behaviors as WT mice, but show impaired modification of behaviors after fear conditioning

In our previous analysis, we compared FrC and Nv mice within each genotype to show that the *Fmr1* KO mice do indeed freeze to a lower extent in the recall period. It remains possible that *Fmr1* KO mice increase another type of "alerting" or "anxious-like" behavior in place of freezing. If this is the case, *Fmr1* KO mice may actually consolidate fear-associated memories as well as WT mice but display this in a way that cannot be measured with standard software used to quantify freezing behavior. Therefore a subset of videos, which were recorded during recall tests, was scored using 7 different observable and distinct behaviors (Table 1). Freezing, scanning and stretch-attend-posture (SAP) are behaviors associated with alerting or fear, whereas motion and rearing are associated with exploratory behavior (Table 1, reviewed in Blanchard, Griebel, Pobbe, & Blanchard, 2011; Roelofs, 2017). For context B, the mice had a layer of bedding on the bottom of the cage and so digging was included in the analysis. Grooming was also scored, but the levels of grooming were so low that these values were taken out of the final analysis. The percentage of total observations was calculated for each animal across these behaviors and a three-way RM ANOVA was conducted with Bonferroni corrected paired comparisons for each recall session. Paired comparisons are reported in text at t-tests. Because the "fear" behaviors and "exploratory" behaviors are potentially opposing types of behavior, they were analyzed separately (Fig. 2).

3.1.2.1. Baseline. During the baseline period both WT and *Fmr1* KO mice spent a large percentage of their time rearing or in motion and

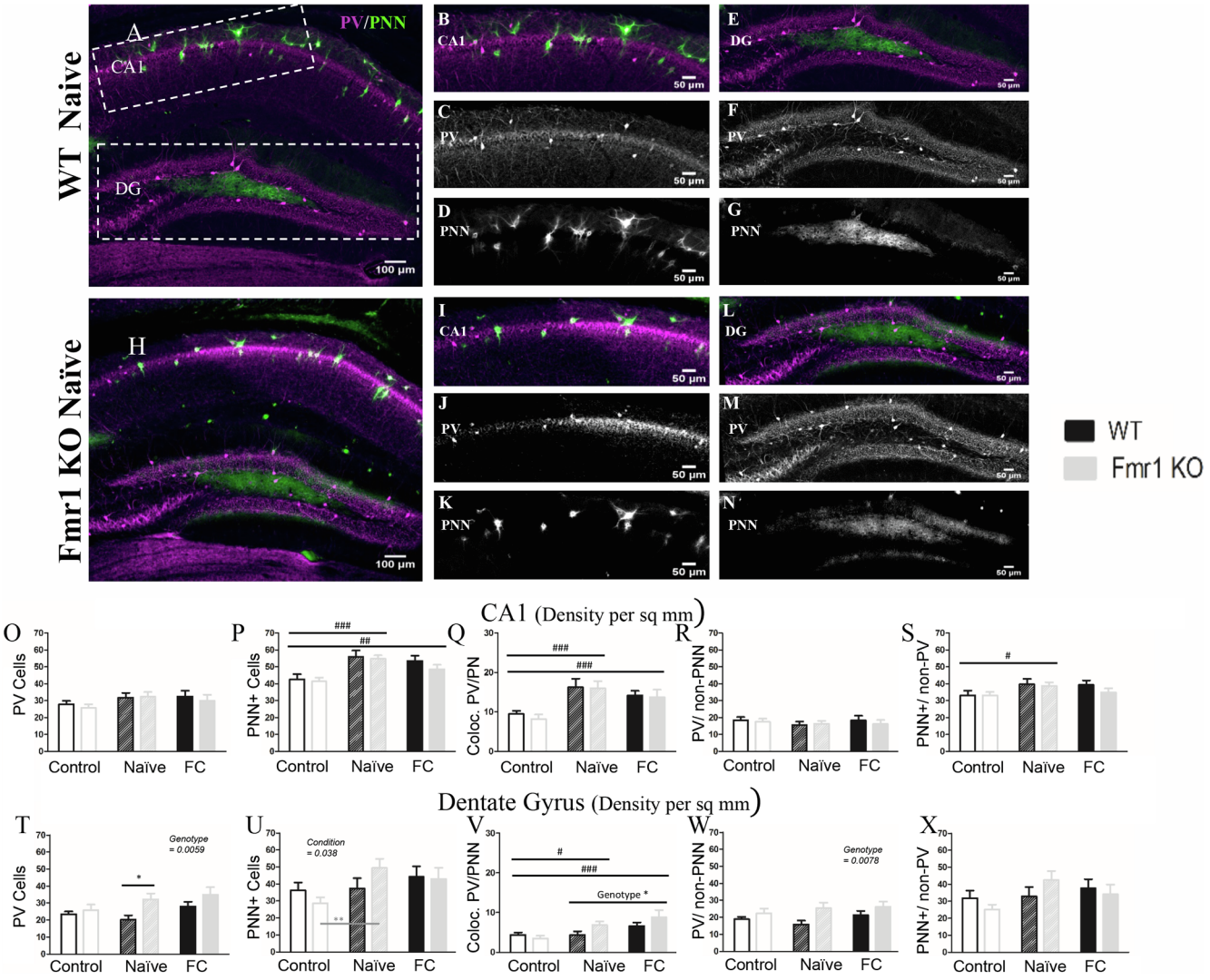

Fig. 5. PV density is elevated in the dentate gyrus of *Fmr1* KO mice but not in the CA1. (A) Example images of coronal sections from a WT naïve and (H) *Fmr1* KO naïve mice. (B), with panels to the right depicting CA1 (B; I) and dentate gyrus (E; L). Panels below CA1 and DG show the PV (C; F; J; M) and PNN (D; G; K; N) channels separately. In CA1 both WT and *Fmr1* KO mice have similar levels of PV (O; R) and PNN (P; S). Both genotypes had increased PNN density in naïve and fear conditioned mice (P). These PNNs were located both around PV cells (Q) and non-PV cells (S). In the DG, there were more PV cells in *Fmr1* KO mice than WT mice (T), both PV cells surrounded by PNN (V) and PV cells without PNNs (W). Similar to CA1 there was increased PNN density in naïve and fear conditioned mice (U), but unlike CA1 the increased PNN seem to be around PV cells (V) and not around non-PV cells (X). Conditioning effect #, ##, ###; paired comparison *, **, *** (p = 0.05, 0.01, 0.001). N per group: WT Nv = 5; WT FrC = 6; WT C = 6, *Fmr1* KO Nv = 6, *Fmr1* KO FrC = 6, *Fmr1* KO C = 5. Image # per group: WT Nv = 16, WT FrC = 17, WT C = 28, *Fmr1* KO Nv = 18, *Fmr1* KO FrC = 16, *Fmr1* KO C = 27.

very little time displaying "fear" behaviors. So in a context that has not been associated with shock, both genotypes show active exploration, even among those mice that underwent fear conditioning 24 h earlier.

3.1.2.2. Tone recall. During tone recall (Fig. 2 row C, Table 5), FrC WT mice significantly reduced the percentage of time spent rearing and motion and increased scanning and freezing behaviors compared to Nv WT mice. FrC *Fmr1* KO mice behaved similarly, decreasing their rearing and increasing both freezing and scanning compared to Nv *Fmr1* KO mice, but their shifts in behavior were attenuated compared to WT mice. Consistent with the 'Freezeframe' analysis, FrC *Fmr1* KO mice froze significantly less than FrC WT mice during tone recall (WT: 31.1%, *Fmr1* KO: 16.1%, t(18) = 3.6, p = 0.0061, r = 0.65, 95% CI [0.84–0.31]).

3.1.2.3. Context recall. During context recall (Fig. 2, row D, Table 5), FrC WT mice decreased the percent of time spent rearing and in motion and increased freezing and scanning compared to Nv WT mice. Again FrC *Fmr1* KO mice had a similar but attenuated shift, reducing their motion and increasing freezing with no change in rearing or scanning compared to Nv *Fmr1* KO mice. When comparing FrC mice across genotypes, *Fmr1* KO mice scanned significantly less than WT (WT: 48.3%; *Fmr1* KO: 31.3%; t(18) = 3.36, p = 0.01, r = 0.62, 95% CI [0.83–0.27]) and displayed more motion (WT: 7.7%; *Fmr1* KO: 24.7%; t (18) = 3.06, p = 0.02, r = 0.58, 95% CI [0.81–0.22]; Fig. 2 row D).

3.1.2.4. Context + tone. During the context + tone test, (Fig. 2 row E, Table 5), FrC WT mice spent the largest percent of their time freezing, with no increase in scanning compared to Nv WT mice, and with close to no time spent in motion or rearing. FrC *Fmr1* KO mice also increased their time spent freezing and decreased the percent of time in motion compared to Nv *Fmr1* KO mice but froze significantly less than FrC WT mice (WT: 57.7%, *Fmr1* KO: 26.2%; t(18) = 5.57, p = 0.000083, r = 0.79, 95% CI [0.91–0.56]; Fig. 2 row E), again supporting the previous analysis. There were few observations of either SAP or digging in either genotype across tests.

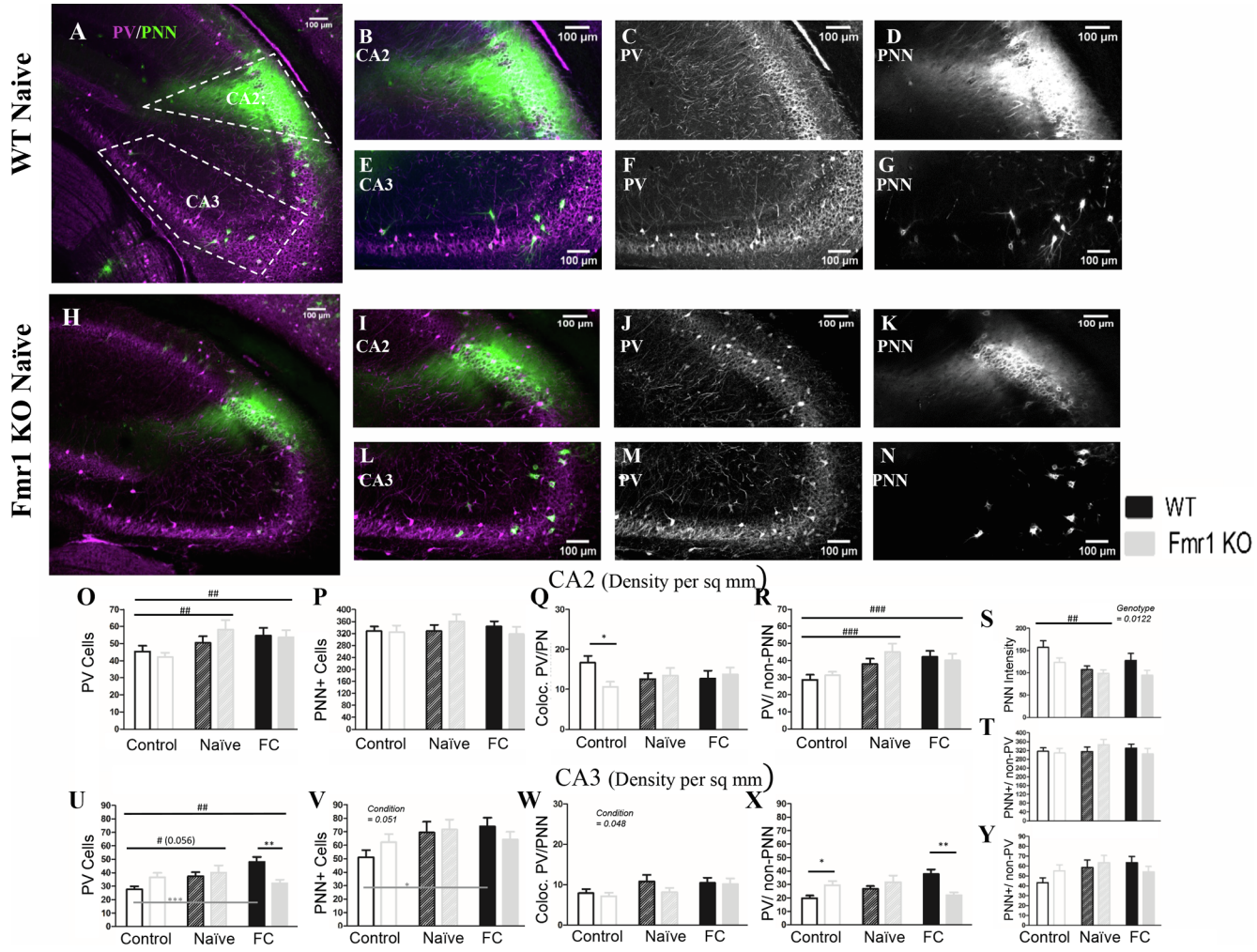

Fig. 6. In CA2 both PV cell density and PNN intensity are modified after conditioning across genotypes; In CA3, PV cell modification is impaired in *Fmr1* KO mice. (A) Example images of a WT naïve coronal slice and (H) an *Fmr1* KO naïve slice, with cropped images of CA2 (B; I) and CA3 (E; L). To the right of the cropped images are PV (C; F; J; M) and PNN (D; G; K; N) channels separated. In CA2 there was no genotype difference in PV density (O) or PNN density (P) between WT and *Fmr1* KO animals. However PV cell density increased (O) in both naïve and fear conditioned mice across genotypes, among PV cells that are not surrounded by PNN (R). We measured WFA fluorescent intensity in CA2 across genotypes and conditioning. Using this metric we found *Fmr1* KO mice have reduced WFA intensity compared to WT mice (S) and a decrease in WFA intensity after conditioning in both genotypes, but no change in PNN density (P; T) or in co-localized PV/PNN cells (Q). In CA3 there was an increase in PV cell density (U) and in PNN cell density (V) in both naïve and fear conditioned mice, which increased the number of co-localized PV/PNN cells (W; fear conditioned only). The increase in PV cells seems to be occurring only in WT mice (U) among PV cells that were not surrounded by PNNs (X). PNNs surrounding non-PV cells showed no change (Y). Conditioning effect #, ##, ###; paired comparison *, **, *** (p = 0.05, 0.01, 0.001). N per group: WT Nv = 5; WT FrC = 6; WT C = 7, *Fmr1* KO Nv = 6, *Fmr1* KO FrC = 6, *Fmr1* KO C = 5. Image # per group: WT Nv = 17, WT FrC = 18, WT C = 32, *Fmr1* KO Nv = 17, *Fmr1* KO FrC = 18, *Fmr1* KO C = 25.

3.1.2.5. Quantification of attenuated behavior. As mentioned above, *Fmr1* KO mice showed appropriate behavioral shifts following conditioning, but their shifts in behavior were attenuated compared to WT mice. We quantified the attenuation by computing a difference score between baseline and recall behavior scores for each animal. The absolute value of the difference of a given behavior was used for further analysis, to account for the fact that freeze/scan/SAP behaviors typically have a positive change from baseline while rearing/motion typically have a negative change. The average of the differences for each animal was compiled and an unpaired *t*-test was run between genotypes. When fear conditioned mice were analyzed in this way, it was confirmed that *Fmr1* KO mice change their behavior less during tone recall ($t(19) = 2.45$, $p = 0.024$, $r = 0.49$, 95% CI [0.75–0.09]), trended toward decreased change during context recall ($t(19) = 1.93$ Welch-corrected, $p = 0.074$, $r = 0.40$, 95% CI [0.71 – (−0.02)]) and during context + tone ($t(19) = 2.00$ Welch-corrected, $p = 0.066$, $r = 0.42$, 95% CI [0.71 – (−0.01)]; Sup. Fig. 2).

Together, these data suggest that *Fmr1* KO mice do not replace immobility with another alerting or anxious-like behavior after fear conditioning. Instead both genotypes respond to fear conditioning with freezing and scanning behaviors during the recall tests, but the *Fmr1* KO response is attenuated compared to WT mice. When the associative cues become more predictive of shock (context + tone), WT mice favor freezing behavior over all others. However, *Fmr1* KO mice responded with a more distributed and attenuated set of behaviors.

3.2. PV and PNN analysis

Parvalbumin protein and mRNA levels can be up- or down-regulated in response to altered neural activity (Cohen et al., 2016; Donato, Rompani, & Caroni, 2013; Favuzzi et al., 2017; Filice, Vörckel, Sungur, Wöhr, & Schwaller, 2016). PNNs are modified after learning events to allow for synaptic reorganization. Thus, changes in PV or PNN density may reflect synaptic or microcircuit reorganization among cells involved in new memory formation/consolidation (Banerjee et al., 2017; Favuzzi et al., 2017). To better understand circuit-level dynamics

Table 2
Details of statistics for behavioral analyses during training. Each section indicates which groups are being compared in statistical analysis. While both WT and *Fmr1* KO mice had low baseline freezing, *Fmr1* KO mice had almost no freezing in Context B leading to a significant difference. Both WT and *Fmr1* KO mice increased freezing across training trials, but *Fmr1* KO mice showed reduced freezing compared to WT mice. Even so, the fear conditioned *Fmr1* KO mice did increase freezing levels after training compared to their naïve counterparts.

	Mean ± SD %		Statistic(df)	Effect Size	95% CI
Habituation	WT FrC	*Fmr1* KO FrC			
Context A	6.91 ± 0.80	5.67 ± 0.67	t(56) = 1.16	r = 0.15	0.39 – (−0.10)
Context B	1.88 ± 0.37	0.69 ± 0.16	t(41) = 2.99**	r = 0.42	0.63–0.15
Training	WT FrC	*Fmr1* KO FrC			
CS-US 1	4.67	4.67			
CS-US 5	74.21	50.52			
	Effect of Training		F(4,224) = 98.03***	η^2 = 0.64	0.69–0.56
	Effect of Genotype		F(1,224) = 23.41***	η^2 = 0.09	0.17–0.03
Training: Nv v FrC	*Fmr1* KO Nv	*Fmr1* KO FrC			
CS-US 5	13.98	50.52	t(46) = 7.29***	r = 0.73	0.84–0.57
	Effect of Training		F(4,184) = 29.98***	η^2 = 0.39	0.47–0.28
	Effect of Condition		F(1,184) = 21.39***	η^2 = 0.10	0.19–0.04

*p = 0.05.
** p = 0.01.
*** p =/ < 0.001.

following fear conditioning, changes in the density of cells expressing PV and PNN were characterized in brain regions associated with context and tone-associated fear memory.

To counterbalance the recall testing during behavior some mice underwent recall testing for the context prior to the tone, whereas others underwent testing of the tone recall prior to the context. Therefore, two separate groups of animals were analyzed based on the order of tone and context recall: (1) tone-context and (2) context-tone. The tone-context experiment is discussed in detail here, with details of context-tone experiments in the supplemental material, because the outcomes were largely similar between the two experiments. The two exceptions to this were CA1 and DG areas that showed notable differences between the two experiments and are discussed here.

3.2.1. Fmr1 removal affected fear conditioning-induced changes in PNNs, but not PV cell density in the auditory cortex

The most consistent deficit we found in *Fmr1* KO mice after fear conditioning is reduced freezing during tone recall, which may indicate changes in auditory cortex processing of sounds and/or altered amygdala function. PV immunoreactivity and PNNs were analyzed in the auditory cortex of Nv and FrC WT and *Fmr1* KO mice. The auditory cortex was divided into superficial (layers 1–4) and deep cortical layers (5–6) for this analysis. A summary of the statistical analyses of auditory cortex data is provided in Table 6.

Both deep and superficial layers showed mostly similar trends in PV immunoreactivity. In superficial layers, PV cell density decreased (p = 0.0056) in both WT and *Fmr1* KO mice after fear conditioning compared to naïve (p = 0.036; Fig. 3F) and to controls (p = 0.0018), indicating PV is down-regulated specifically in response to fear conditioning. In deep layers, PV cell density decreased moderately (p = 0.062) in FrC mice compared to control mice (p = 0.02; Fig. 3K) but did not change relative to Nv mice (p = 0.74). Genotype had no effect on PV cell density (superficial layers: p = 0.71; deep layers: p = 0.60). In both deep and superficial layers, the observed overall reduction in PV cell density was due to the loss of PV cells lacking PNNs (superficial layers: C v FrC: p = 0.0006; Nv FrC: p = 0.026; deep layers:

Table 3
Details of statistics for behavioral analyses during testing. *Fmr1* KO mice froze less than WT mice during Tone recall and Context + Tone recall. Compared to their naïve counterparts, *Fmr1* KO mice that were fear conditioned did not show increased freezing during Tone recall, indicating a Tone recall deficit.

	Mean ± SD %		Statistic(df)	Effect Size	95% CI
Recall (24 h)					
RM ANOVA- all tests	Effect of Test		F(3, 300) = 197.04***	η^2 = 0.66	0.71–0.60
	Effect of Genotype		F(1,100) = 20.35***	η^2 = 0.17	0.30–0.05
	Effect of Condition		F(1, 100) = 110.68***	η^2 = 0.52	0.62–0.39
	Interaction		F(1,100) = 6.02*	η^2 = 0.06	0.16–0.001
WT v *fmr1* KO	WT FrC	*Fmr1* KO FrC			
Baseline	1.21	0.53	t(56) = 0.15	r = 0.02	0.27 – (−0.23)
Tone	22.20 ± 2.71	5.91 ± 1.15	t(56) = 3.70 **	r = 0.44	0.63–0.21
Context	37.48 ± 3.88	27.39 ± 4.53	t(56) = 2.29	r = 0.29	0.51–0.042
Context + Tone	75.00 ± 3.65	50.31 ± 4.37	t(56) = 5.61 ***	r = 0.60	0.74–0.41
Nv v FrC	WT Nv	WT FrC			
Tone	3.51	22.20	t(54) = 3.98 ***	r = 0.48	0.65–0.25
Context	16.46	37.48	t(56) = 4.47 ***	r = 0.52	0.69–0.30
Context + Tone	17.40	75.00	t(56) = 12.26 ***	r = 0.86	0.91–0.77
	Fmr1 KO Nv	*Fmr1* KO FrC			
Tone	1.30	5.91	t(46) = 1.1	r = 0.16	0.42 – (−0.12)
Context	10.75	27.39	t(46) = 3.98 ***	r = 0.51	0.84–0.27
Context + Tone	11.60	50.31	t(46) = 9.27 ***	r = 0.81	0.89–0.68

* p = 0.05.
** p = 0.01.
*** p = < 0.001.

Table 4
Comparison of high-freezing *Fmr1* KO mice only. Even when accounting for *Fmr1* KO mice that froze to low levels during fear conditioned training, *Fmr1* KO mice still froze significantly less during Tone recall and Context + Tone recall compared to WT mice.

	Mean %		Statistic(df)	Effect Size	95% CI
Hi Freezers: Training					
	WT FrC	*Fmr1* KO FrC			
CS-US 4	58.40	54.03	t(44) = 0.68	r = 0.10	0.37–0.19
CS-US 5	74.21	71.64	t(44) = 0.40	r = 0.06	0.34 – (−0.23)
Hi Freezers: Recall					
	WT FrC	*Fmr1* KO FrC			
Tone	22.2	8.5	t(44) = 2.61*	r = 0.36	0.59–0.09
Context	37.5	28.5	t(44) = 1.71	r = 0.25	0.49 – (−0.037)
Context + Tone	75	51.7	t(44) = 4.43***	r = 0.55	0.72–0.32

**p = 0.01.
* p = 0.05.
** p = < 0.001.

C v FrC: p = 0.0009; Fig. 3I and N). There was no difference in density of PV cells with PNN either in superficial (p = 0.68) or in deep layers (p = 0.84).

Unlike PV density, PNN density was lower overall in *Fmr1* KO mice compared to WTs (superficial layers: p = 0.0015; deep layers: p = 0.0012; Fig. 3G and L), replicating previous findings in young mice (Wen, Afroz, et al., 2018). Reduced PNNs in *Fmr1* KO mice were observed around non-PV cells (superficial layers: p = 0.046; deep layers: p = 0.019; Fig. 3J and O), but no genotype difference was seen in density of PNNs around PV cells (superficial layers: p = 0.21; deep layers: p = 0.28; Fig. 3H and M).

In deep layers, PNN density was increased (p = 0.016) in FrC mice compared to control mice (p = 0.04) and to a lesser degree in Nv mice compared to control mice (p = 0.056). In superficial layers, there was a change in PNN density (p = 0.0013). In this case PNN density increased in WT Nv mice compared to controls (Nv v C: p = 0.0002), but was lower in WT FrC mice compared to WT Nv mice (WT: C: 108.4, Nv: 143.2; FrC: 120.8; Nv v FrC: p = 0.013); however PNN density was not modified in *Fmr1* KO mice (*Fmr1* KO: C: 104; Nv: 109.4; FrC: 116.4).

Together, the data show impaired PNN density in *Fmr1* KO mice compared to WT mice in the auditory cortex. In contrast, PV cell density was similar across genotypes, and fear conditioning induced a decrease in PV cell density in both WT and *Fmr1* KO mice. This was mainly seen in PV cells lacking PNNs. We also observed layer-specific differences in PNN regulation in WT mice and between genotypes, suggesting that (1) PNNs are differentially regulated in different cortical layers and (2) PNN changes induced by tone fear conditioning in the superficial layers of WT mice were impaired in *Fmr1* KO mice compared to WT mice.

3.2.2. PNN density is reduced in the amygdala of Fmr1 KO mice

We focused on the lateral and basolateral nuclei of amygdala, which are readily identifiable and involved in fear-associative memory formation. A summary of the statistical analyses of amygdala data is provided in Table 7. Neither the lateral or basolateral amygdala showed genotype differences in overall PV cell density (Lateral: p = 0.52; Basolateral: p = 0.44; Fig. 4J and O; Fig. 7) or showed an effect of fear conditioning (Lateral: p = 0.66; Basolateral: p = 0.13). However, a significant reduction in the density of PV cells lacking PNNs was observed in basolateral amygdala after conditioning (p = 0.046; Fig. 4R).

In both lateral and basolateral amygdala, there were significantly fewer PNNs in *Fmr1* KO mice than in WT mice (Lateral: p < 0.0001; Basolateral: p = 0.0062; Fig. 4K and P), specifically fewer PNNs around non-PV cells (Lateral: p = 0.0001; Basolateral: p < 0.0001; Fig. 4N and S). There was no genotype difference in density of PV cells containing PNNs (Lateral: p = 0.23; Basolateral: p = 0.77; Fig. 4L and Q). These data show a baseline deficit in PNN formation in the amygdala of *Fmr1* KO mice, compared to WT mice.

In both genotypes, PNN density was upregulated after training both in the lateral amygdala (p < 0.0001; C vs. Nv: p < 0.0003; FrC vs. C: p = 0.003) and in the basolateral amygdala (p = 0.0004; C vs. Nv:

Table 5
Behavioral analysis of *Fmr1* KO and WT mice during recall tests. All statistics here are comparisons between naïve and fear conditioned mice of the same genotype. Although *Fmr1* KO mice show similar shifts in behavior after fear conditioning, these changes are consistently less pronounced than in WT mice.

	% (r effect size [95% CI])					
	WT			*Fmr1* KO		
Tone						
Non-Fear	Naive	Fear Conditioned		Naive	Fear Conditioned	
Rearing	**31.1**	**8.8**	***(0.74 [0.89–0.47])	**48.7**	**16.6**	***(0.85 [0.93–0.66])
Motion	**33.3**	**15**	**(0.68 [0.85–0.36])	**24.7**	**24.7**	
Fear						
Scanning	**18.3**	**35.5**	**(0.69 [0.86–0.38])	**11.7**	**28.2**	**(0.67 [0.85–0.35])
Freezing	**5**	**31.1**	***(0.82 [0.92–0.61])	**3**	**16.1**	*(0.58 [0.81–0.22])
Context						
Non-Fear	Naive	Fear Conditioned		Naive	Fear Conditioned	
Rearing	**20.5**	**2.7**	*(0.59 [0.81–0.23])	**24.1**	**11.1**	
Motion	**34.4**	**7.7**	***(0.74 [0.89–0.47])	**40.1**	**24.7**	*(0.54 [0.78–0.15])
Fear						
Scanning	**29.4**	**48.3**	**(0.65 [0.84–0.32])	**24.7**	**31.3**	
Freezing	**7.7**	**26.6**	**(0.65 [0.84–0.32])	**4.3**	**18.6**	*(0.54 [078–0.16])
Context + Tone						
Non-Fear	Naive	Fear Conditioned		Naive	Fear Conditioned	
Rearing	**26.1**	**0.0**	**(0.69 [0.86–0.38])	**27.2**	**13.1**	
Motion	**33.3**	**2.8**	***(0.75 [0.89–0.47])	**31.5**	**14.6**	*(0.52 [0.77–0.13])
Fear						
Scanning	**30.5**	**36.1**	*ns* (0.22 [0.59 – (−0.22)])	**26.5**	**33.8**	
Freezing	**57.7**	**3.8**	***(0.91 [0.96–0.79])	**4.9**	**26.2**	**(0.65 [0.84–0.32])

* p = 0.05.
** p = 0.01.
*** p < 0.001.

Table 6
Details of statistics for PV, PNN and PV/PNN density in auditory cortex.

A1 Cell Density	Main Effect	Statistic (df)	Effect Size (η^2)	95% CI	2-Cond Test (η^2 effect size)
PV					
Superficial	Conditioning	F(2,100) = 5.47, p = 0.0056	0.10	0.21–0.01	FrC v Nv* (0.08) FrC v C** (0.17)
	Genotype	F(1,100) = 0.13, p = 0.71	0.001	0.05–0.0	
Deep	Conditioning	F(2,100) = 2.85, p = 0.062	0.05	0.15–0.0	FrC v Nv (0.02) FrC v C* (0.11)
	Genotype	F(1,100) = 0.27, p = 0.60	0.003	0.05–0.0	
PNN					
Superficial	Conditioning	F(2,100) = 7.07, p = 0.0013	0.12	0.24–0.02	**WT only** C v Nv*** (0.62) FrC v Nv* (0.46)
	Genotype	F(1,100) = 10.6, p = 0.0015	0.09	0.21–0.01	
Deep	Conditioning	F(2,100) = 4.28, p = 0.016	0.07	0.18–0.0	C v Nv* (0.08) FrC v C* (0.09)
	Genotype	F(1,100) = 11.11, p = 0.0012	0.10	0.22–0.02	
PV + PNN +					
Superficial	Conditioning	F(2,100) = 0.38, p = 0.68	0.007	0.05–0.0	
	Genotype	F(1,100) = 1.61, p = 0.21	0.01	0.09–0.0	
Deep	Conditioning	F(2,100) = 0.18, p = 0.84	0.003	0.04–0.0	
	Genotype	F(1,100) = 1.16, p = 0.28	0.01	0.08–0.0	
PV − PNN +					
Superficial	Conditioning	F(1,100) = 4.1, p = 0.046	0.04	0.13–0.0	
Deep	Conditioning	F(1,100) = 5.65, p = 0.019	0.05	0.16–0.0	
PV + PNN −					
Superficial					FrC v Nv* (0.09) FrC v C*** (0.19)
Deep					FrC v C*** (0.18)

* p = 0.05.
** p = 0.01.
*** p < 0.001.

p = 0.0042; C vs. FrC: p = 0.0006). This upregulation of PNNs seemed to occur around both PV cells (Lateral: p = 0.0001; Basolateral: p = 0.0043), and non-PV cells (Lateral: p = 0.027; Basolateral: p = 0.013). However, no difference was observed in PNN density between Nv and FrC mice, suggesting changes in PNN density are not specifically due to fear conditioning alone.

Table 7
Details of statistics for PV, PNN and PV/PNN density in the amygdala.

Amygdala Cell Density	Main Effect	Statistic (df)	Effect Size (η^2)	95% CI	2-Cond Test (η^2 effect size)
PV					
Lateral	Conditioning	F(2,92) = 0.41, p = 0.66	0.009	0.06–0.0	
	Genotype	F(1,92) = 0.42, p = 0.52	0.004	0.07–0.0	
Basolateral	Conditioning	F(2,92) = 2.06, p = 0.13	0.04	0.13–0.0	
	Genotype	F(1,92) = 0.61, p = 0.44	0.006	0.07–0.0	
PNN					
Lateral	Conditioning	F(2,92) = 11.62, p < 0.0001	0.20	0.33–0.06	C v Nv*** (0.26) C v FrC** (0.16)
	Genotype	F(1,92) = 18.1, p < 0.0001	0.16	0.30–0.05	
Basolateral	Conditioning	F(2,92) = 8.42, p = 0.0004	0.15	0.28–0.03	C v Nv** (0.16) C v FrC*** (0.20)
	Genotype	F(1,92) = 7.86, p = 0.0062	0.08	0.20–0.0	
PV + PNN +					
Lateral	Conditioning	F(2,92) = 9.95, p = 0.0001	0.18	0.30–0.05	
	Genotype	F(1,92) = 1.43, p = 0.23	0.01	0.1–0.0	
Basolateral	Conditioning	F(2,92) = 5.78, p = 0.0043	0.11	0.23–0.01	
	Genotype	F(1,92) = 0.09, p = 0.77	0.001	0.05–0.0	
PV − PNN +					
Lateral	Conditioning	F(2,92) = 3.74, p = 0.027	0.07	0.18–0.0	
	Genotype	F(1,92) = 16.42, p = 0.0001	0.15	0.28–0.04	
Basolateral	Conditioning	F(2,92) = 4.59, p = 0.013	0.09	0.20–0.0	
	Genotype	F(1,92) = 19.17, p < 0.0001	0.17	0.30–0.05	
PV + PNN −					
Lateral	No effects				
Basolateral	Conditioning	F(2,92) = 3.18, p = 0.046	0.06	0.17–0	

* p = 0.05.
** p = 0.01.
*** p < 0.001.

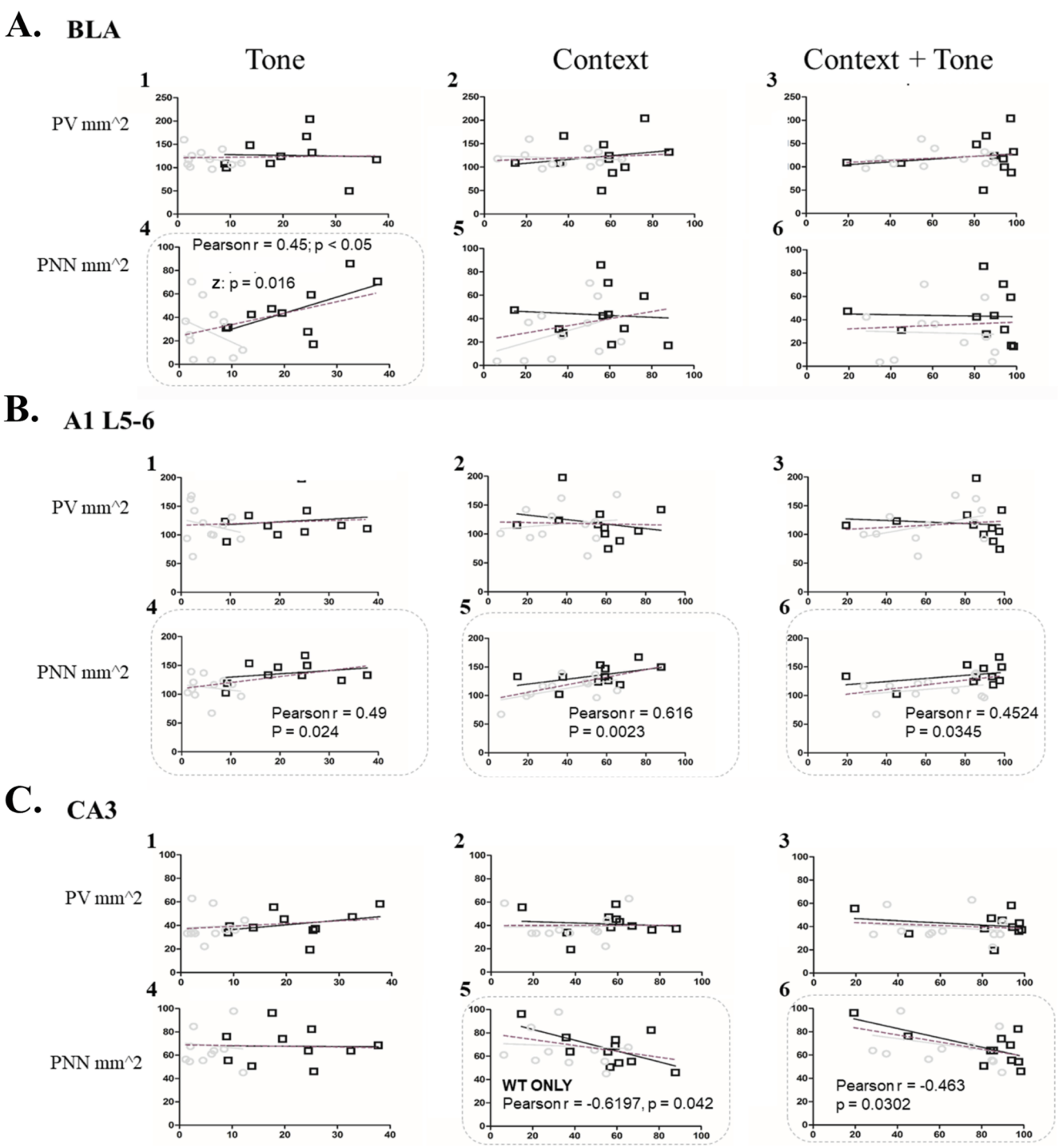

Fig. 7. High PNN density is correlated with higher freezing behavior across multiple brain regions. Panel A shows basolateral amygdala, Panel B deep layers of auditory cortex and Panel C shows CA3. Each column shows the correlation between an animal's freezing during a recall test (Tone, Context or Context-with-Tone) and their levels of PV cell density (1–3) or PNN density (4–6). In both deep A1 and basolateral amygdala high freezing during tone recall was correlated with higher levels of PNN density. Additionally, in both deep A1 and CA3, high freezing during context or context-with-tone recall was correlated with high PNN levels. KEY: The grey line indicates *Fmr1* KO regression curve, black line indicates WT regression curve, and the dotted line indicates the genotypes grouped. Pearson's r indicates correlation when both genotypes are grouped. Z indicates the difference between the Pearson's r values for WT and *Fmr1* KO mice on a Z-scale.

Thus in the amygdala, similar to the AC, reduced PNNs, but not PV cell density, was observed in *Fmr1* KO mice compared to WT mice. In contrast to AC, in the amygdala, we saw no changes in PV cell density following fear conditioning, whereas PNN density increased in both Nv and FrC mice, suggesting that these changes in PNNs may represent modifications due to context exposure instead of fear conditioning.

3.2.3. No genotype differences were observed in PV and PNN cell densities in CA1 hippocampus

A summary of the statistical analyses of CA1 region is provided in Table 8. The CA1 showed no genotype differences in PV density ($p = 0.53$; Fig. 8) or differences due to conditioning ($p = 0.077$; Fig. 5O). PNN density was also not different between WT and *Fmr1* KO mice ($p = 0.32$). However, PNN density was modified after

Table 8
Details of statistics for PV, PNN and PV/PNN density in CA1 of the hippocampus.

CA1 Cell Density	Main Effect	Statistic (df)	Effect Size (η^2)	95% CI	2-Cond Test (η^2 effect size)
PV					
	Conditioning	F(2,116) = 2.61, p = 0.077	0.04	0.12–0	
	Genotype	F(1,116) = 0.39, p = 0.53	0.003	0.05–0	
PNN					
	Conditioning	F(2,116) = 12.15, p < 0.0001	0.17	0.28–0.06	C v Nv*** (0.19) C v FrC** (0.10)
	Genotype	F(1,116) = 0.98. p = 0.32	0.008	0.07–0	
PV + PNN +					
	Conditioning	F(2,116) = 15.11, p < 0.0001	0.21	0.32–0.08	
PV-PNN +					
	Conditioning	F(2,116) = 3.06, p = 0.05	0.05	0.13–0	

*p = 0.05.
** p = 0.01.
*** p < 0.001.

conditioning (p < 0.0001) increasing in both Nv (Nv v C: p < 0.0003) and FrC mice (FrC v C: p = 0.0078) compared to controls (Fig. 5P). This increase in PNNs occurs around both PV (p < 0.0001; Fig. 5Q) and non-PV cells (p = 0.05; Fig. 5S), and as in the amygdala, indicates PNN modifications that are not specific to the fear conditioning.

Although the tone-context experiment showed no modifications in PV or PNN cell density between Nv and FrC mice (as discussed above), the context-tone experiment (data in supplemental material) showed a decrease in PV density (p = 0.0033) in FrC compared to Nv mice in both genotypes (Sup. Fig. 3A), mainly in PV cells with PNNs (p = 0.0058; Sup. Fig. 3C), but with a trend towards reduced PV density among PV cells without PNNs (p = 0.055). The context-tone experiment also showed opposing changes in PNN density between genotypes. WT mice showed no change in PNN density after FrC (WT Nv: 39.93; FrC: 45.38; t(41) = 1.02, p = 0.94, r = 0.16, 95% CI [0.43 – (−0.14)]) whereas FrC *Fmr1* KO mice had decreased PNN density compared to Nv mice (*Fmr1* KO Nv: 55.27; FrC: 38.93; t(40) = 3.03, p = 0.013, r = 0.43, 95% CI [0.65–0.15]; Sup. Fig. 3B). If we compare this to controls (shown in Fig. 5; WT C: 42.58; *Fmr1* KO C: 41.34), it is apparent that WT mice had no changes in PNN density in Nv and FrC

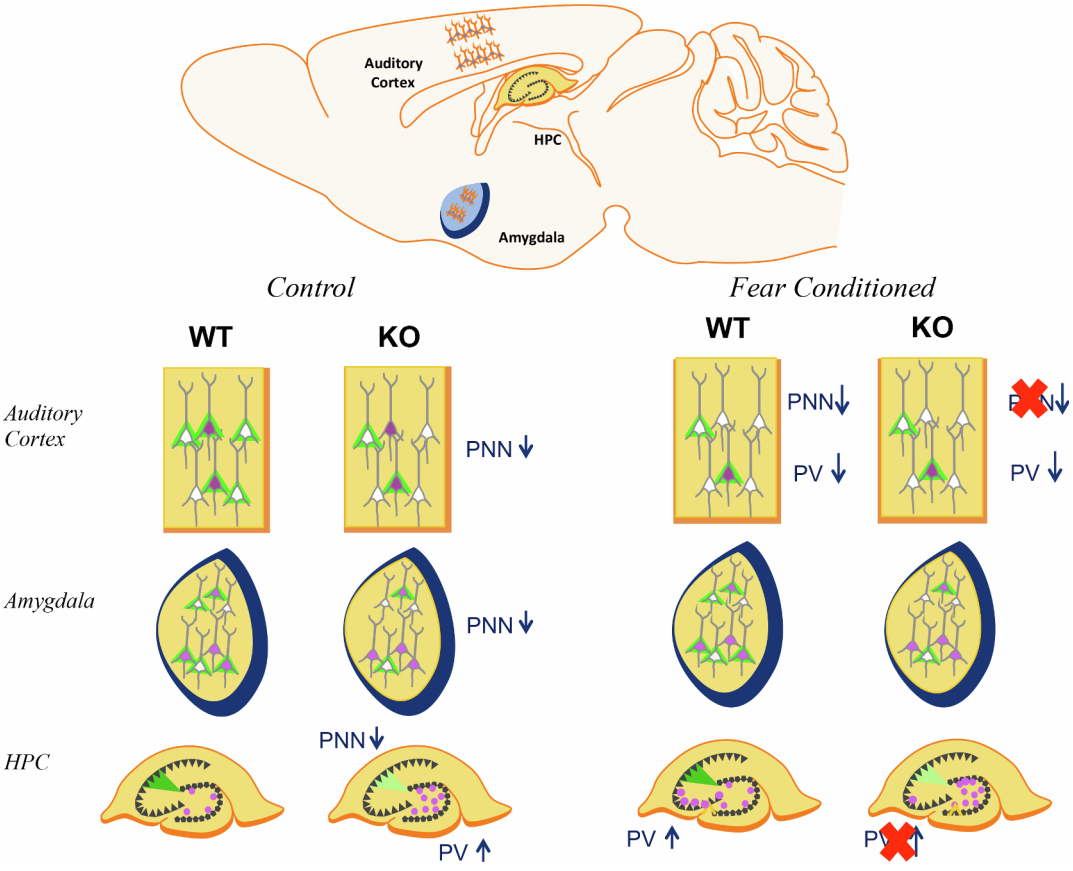

Fig. 8. Summary of Results. In control conditions, *Fmr1* KO mice have reduced PNN density in the auditory cortex and amygdala as well as reduced PNN intensity in CA2. Conversely, PV cell density is increased in DG of *Fmr1* KO mice. After fear conditioning, WT mice had decreased PV cell density and decreased PNN density in the auditory cortex (superficial layers) as compared to naïve mice. *Fmr1* KO mice did not show PNN modulation in the AC (FrC vs N). In the CA3 hippocampus, FrC WT mice showed an increase in PV density in CA3 compared to controls, which was impaired in *Fmr1* KO mice.

mice as compared to controls, whereas *Fmr1* KO mice showed an up-regulation in Nv mice compared to controls (Nv vs. C paired comparison: t(46) = 2.937, p = 0.015, r = 0.40, 95% CI [0.61–0.13]) which was downregulated in FrC mice.

Differences in PV and PNN between experiments in the CA1 may reflect modification of the contextual memory after re-exposure to the training contexts during recall tests. This is consistent with the role of the dorsal hippocampus in contextual memory formation. The differences in time between context recall and tissue collection in the two experiments, context-tone (4 h) versus tone-context (30 min), likely reflects modification of PV and PNN on different timescales post-recall. 4 h after re-exposure to the context there is down-regulation of PV expression in CA1 of all FrC mice, and differential regulation of PNN density between WT and *Fmr1* KO mice.

3.2.4. PV cell density is increased in the dentate gyrus of Fmr1 KO mice

The dentate gyrus (DG) is the main input region of the hippocampus. A summary of the statistical analyses of DG region is provided in Table 9. In contrast to the findings in the AC, amygdala and CA1, the dentate gyrus (DG; Table 9) showed elevated density of PV cells in *Fmr1* KO mice compared to WT mice (p = 0.0059; Fig. 5T), consisting mainly of PV cells without PNNs (p = 0.0078; Fig. 5V) but no change in PV cells with PNNs (p = 0.098; Fig. 5W).

Similar to amygdala, PNN density changed in the DG after conditioning (p = 0.038; Fig. 5U). Paired comparisons show that naïve *Fmr1* KO mice had increased PNNs compared to controls (C vs. Nv: p = 0.016; *Fmr1* KO: C: 28.63; Nv: 49.33; FrC: 42.93) but this was not observed in WT mice (C vs. Nv: p = 0.88; WT: C: 36.21; Nv: 37.31; FrC: 44.15). There was no significant difference in PNN density between genotypes (p = 0.80). Conditioning-induced increase in PNNs was mainly observed around PV cells (p = 0.0003; Fig. 5V) whereas the density of non-PV cells with PNNs did not change following conditioning (p = 0.096; Fig. 5X).

Similar to CA1, the DG showed differences between the tone-context experiment (discussed above) and the context-tone experiment (supplemental material). In the context-tone experiment there was an overall effect of conditioning on PV cell density (p = 0.022), with reduced PV cell density in FrC mice compared to Nv mice, which was largely due to reduced PV density in *Fmr1* KO mice but not in WT mice (WT: Nv: 40.85, FrC: 41.92; *Fmr1* KO: Nv: 50.58; FrC: 35.49; Sup. Fig. 3Q). When these data are compared to controls from Fig. 5 (WT C: 23.4; *Fmr1* KO C: 25.87), it is clear that both WT (C vs. Nv: p = 0.0001; C vs. FrC: p = 0.000063) and *Fmr1* KO mice (C vs. Nv: p = 0.00000076; C vs. FrC: p = 0.06) upregulate PV density in Nv and FrC conditions compared to C mice, but *Fmr1* KO mice then decrease PV density after fear conditioning (Nv vs. FrC: p = 0.005) whereas WT do not (Nv vs. FrC: p = 0.80).

PNN density was also different between experiments and showed differential regulation in WT and *Fmr1* KO mice, similar to observations in CA1. PNN density increased in WT mice after fear conditioning (FrC v C: p = 0.055), while PNN was not changed in *Fmr1* KO mice (p = 0.53), leading to significantly fewer PNNs in FrC *Fmr1* KO mice (p = 0.032) compared to FrC WT mice (WT: Nv: 20.22, FrC: 32.53, *Fmr1* KO: Nv: 25.18, FrC: 17.81; Sup. Fig. 3R). Comparing these data to controls from Fig. 5, (WT: C: 36.21; *Fmr1* KO: C: 28.63), it becomes clear that Nv WT mice actually downregulate PNN compared to controls (WT Nv v C: p = 0.014), but no difference is detected in FrC WT mice compared to WT controls, whereas *Fmr1* KO mice do not show PNN regulation (*Fmr1* KO Nv v C: p = 0.54). Together, these results suggest that PV and PNN are not being regulated in the same way in the DG of WT and *Fmr1* KO mice. PV levels are higher and fluctuate more in *Fmr1* KO mice than in WT mice. Comparison between tone-context and context-tone experiments suggest that regions of the hippocampus necessary for maintaining the contextual memory component of fear conditioning (CA1 and DG) undergo time-dependent changes in PV and PNN cell density that are different between genotypes.

3.2.5. PNN intensity in CA2 is reduced in Fmr1 KO mice

The CA2 has a region of high PNN expression. WFA labeling extends from the stratum pyramidale of CA2 to the dorsal granule cell layer of the dentate gyrus, potentially dendrites of CA2 neurons. As this labeling of fluorescently tagged WFA is profuse and far outside the stratum pyramidale, we measured PNN intensity in CA2 in addition to counting PNN positive cells. A summary of the statistical analyses of CA2 region is provided in Table 10. The WFA fluorescence intensity was reduced in *Fmr1* KO mice compared to WT mice (p = 0.021; Fig. 6S; Table 10). Conditioning affected WFA fluorescence intensity (p = 0.0084) by decreasing fluorescence intensity in Nv mice compared to controls (Nv v C: p = 0.0063). However, Nv and FrC mice were not different from each other. PNN levels remained low in *Fmr1* KO mice under all conditions. Although WFA fluorescence intensity decreased, PNN cell density was not different between genotypes (p = 0.97) or in response to conditioning (p = 0.69, Fig. 6P).

PV density increased after conditioning (p = 0.0052]) in both naïve (Nv v C: p = 0.02) and fear conditioned mice (FrC v C: p = 0.015) compared to controls (Fig. 6O) with no genotype differences (p = 0.72). Together these results suggest reduced PNN and an increase in PV expression after both naïve and fear conditioning, but no specific effect of fear conditioning alone in the CA2.

Table 9
Details of statistics for PV, PNN and PV/PNN density in the dentate gyrus of the hippocampus.

DG Cell Density	Main Effect	Statistic (df)	Effect Size (η^2)	95% CI	2-Cond Test (η^2 effect size)
PV					
	Genotype	F(1,116) = 7.88, p = 0.0059	0.06	0.16–0.0	
PNN					
	Conditioning	F(2,116) = 3.35, p = 0.038	0.05	0.14–0.0	***Fmr1* KO only** C v Nv*** (0.40)
	Genotype	F(1,116) = 0.06, p = 0.80	0.0005	0.03–0.0	
PV + PNN +					
	Conditioning	F(2,116) = 8.59, p = 0.0003	0.13	0.24–0.03	
	Genotype	F(1,116) = 2.77, p = 0.098	0.02	0.09–0.0	
PV + PNN −					
	Genotype	F(1,116) = 7.33, p = 0.0078	0.06	0.16–0.0	
PV − PNN +					
	Conditioning	F(2,116) = 2.39, p = 0.096	0.04	0.12–0.0	

*p = 0.05.
**p = 0.01.
*** p < 0.001.

Table 10
Details of statistics for PV, PNN and PV/PNN density in CA2 of the hippocampus.

CA2 Cell Density	Main Effect	Statistic (df)	Effect Size (η^2)	95% CI	2-Cond Test (η^2 effect size)
PV					
	Conditioning	F(2,121) = 5.49, p = 0.0052	0.08	0.18–0.0	C v Nv* (0.08) C v FrC* (0.08)
	Genotype	F(1,121) = 0.13, p = 0.72	0.001	0.04 0.0	
PNN intensity					
	Conditioning	F(2,108) = 4.99, p = 0.0084	0.08	0.18–0.0	C v Nv** (0.12)
	Genotype	F(1,108) = 5.44, p = 0.021	0.05	0.14–0.0	
PNN					
	Conditioning	F(2,121) = 0.37, p = 0.69	0.006	0.05–0.0	
	Genotype	F(1,121) = 0.0016, p = 0.97	0.00001	0.004–0.0	

*** p < 0.001.
* p = 0.05.
** p = 0.01.

3.2.6. PV cell density in CA3 increases after conditioning in WT but not in *Fmr1* KO mice

A summary of the statistical analyses of CA3 region is provided in Table 11. PV cell density in the CA3 increases after fear conditioning (p = 0.026; Table 11) in FrC mice when compared to control mice (FrC v C: p = 0.021), but not compared to Nv mice (FrC v Nv: p = 0.69). This increase seems to be carried by WT mice (WT C: 27.78, WT FrC: 48.15C vs. FrC: p = 0.000096). Because *Fmr1* KO levels do not change (*Fmr1* KO C: 36.69, *Fmr1* KO FrC: 32.25; *ns*) but WT levels increase, this leads to significantly more PV in FrC WT mice compared to FrC *Fmr1* KO mice (p = 0.008). However, the main effect of genotype shows no overall difference in PV cell density between genotypes (p = 0.59; Fig. 6U). We also observed a specific reduction in density of PV cells without PNNs in FrC *Fmr1* KO mice compared to FrC WTs (p = 0.004; Fig. 6X).

PNN cell density is also altered in CA3 hippocampus after conditioning (p = 0.051; Fig. 6V), carried by an up-regulation of PNNs in WT FrC compared to C mice (p = 0.037) with no significant changes between FrC and C *Fmr1* KO groups (p = 0.83). We also observed an increase in the density of PV cells with PNNs after fear conditioning (p = 0.048; Fig. 6W) in both WT and *Fmr1* KO mice, but no change in PNNs surrounding non-PV cells (p = 0.11; Fig. 6Y).

Overall, CA3 shows an increase in PV and PNN cell density in WT mice after fear conditioning which is attenuated or absent in *Fmr1* KO mice. However, density of PV cells with PNNs was upregulated in both WT and *Fmr1* KO mice following FrC. These effects cannot be attributed solely to fear conditioning, as FrC and Nv mice were not different from each other.

3.3. Correlations between mouse behavior and PV/PNN expression

3.3.1. PNN density in AC and amygdala correlate with the strength of the tone-associated memory

To further understand the relationship between changes in molecular markers of plasticity and the mouse freezing behaviors during fear recall, we examined the correlation between the PV density, PNN density and PV/PNN co-localization with the three recall tests in FrC WT and *Fmr1* KO mice. This correlation could only be run on the subset of mice used for tissue collection (n = 11 wt, 11 *Fmr1* KO); including context-tone and tone-context experiments; therefore the training and recall data for these mice is provided in Supplemental Fig. 1C and D. We combined both genotypes to assess the overall relationship between behavior and cellular changes, and also generated a regression curve for each genotype separately to compare the curves and correlation values between WT and *Fmr1* KO mice.

There was a positive correlation in the basolateral amygdala for tone recall (tone: r = 0.45, p < 0.05; Fig. 7A4) when all mice were included. When WT and *Fmr1* KO mouse data were separated, the correlation coefficients between genotypes were different from each other (Z = −2.14: p = 0.016). Freezing in WT mice was positively correlated with PNN (r = 0.62) but freezing in *Fmr1* KO mice was negatively correlated (r = −0.34). This same overall relationship with PNN density was found in auditory cortex (deep layers) between the density of PNNs and the strength of freezing during all recall tests when all mice are combined, where mice that freeze more tend to have higher PNN density (tone: r = 0.49, p = 0.024; context: r = 0.62, p = 0.0023; context + tone: r = 0.45, p = 0.035; Fig. 7B4–6). When WT and *Fmr1* KO mice were separated and compared, the correlation coefficients of

Table 11
Details of statistics for PV, PNN and PV/PNN density in CA3 of the hippocampus.

CA3 Cell Density	Main Effect	Statistic (df)	Effect Size (η^2)	95% CI	2-Cond Test (η^2 effect size)
PV					
	Conditioning	F(2,117) = 3.75, p = 0.026	0.06	0.15–0	C v FrC* (0.08)
	Genotype	F(1,117) = 0.29, p = 0.59	0.002	0.05–0	
PNN					
	Conditioning	F(2,117) = 3.04, p = 0.051	0.05	0.13–0	C v FrC* (0.36)
PV + PNN +					
	Conditioning	F(2,117) = 3.1, p = 0.048	0.05	0.13–0	
PV − PNN +					
	Conditioning	F(2,117) = 2.27, p = 0.11	0.04	0.11–0	

** p = 0.01
*** p < 0.001.
* p = 0.05.

each genotype were not different from each other. Taken together, it appears that in WT mice there is an increase in PNNs after fear conditioning in both basolateral amygdala and the deep layers of AC, and this increase is correlated with the strength of freezing during tone recall. *Fmr1* KO mice, which have consistently low freezing to the tone and reduced PNNs, do not show a relationship between PNN density and freezing during tone recall.

3.3.2. PNN in CA3 is correlated with the strength of the contextual memory

On data combining the two genotypes, the CA3 showed a negative correlation between PNN density and the amount of freezing during context + tone recall, where mice that tended to freeze more also showed less PNN (context + tone: $r = -0.46$, $p = 0.03$, genotype grouped; Fig. 7C6). Freezing during context recall (without a tone) was also negatively correlated with PNN density in WT mice only ($r = -0.62$, $p = 0.042$; Fig. 7C5) but not in *Fmr1* KO mice ($r = -0.07$, ns) strengthening the idea that WT mice modify PNN density after fear conditioning.

3.4. Additional analyses of PV and PNN intensity and cell counts with the PIPSQUEAK method

Additional analysis of PV/PNN was performed using the PIPSQUEAK method, a standardized and semi-automatic procedure that provides information on both cell counts and intensity of PV and PNN labeling (Slaker, Barnes, et al., 2016; Slaker, Blacktop, et al., 2016; Slaker, Harkness, et al., 2016). The PIPSQUEAK analyses of cell density were not significantly different from the original results using ImageJ (Sup. Tables). The intensity analysis showed that in the auditory cortex (Sup. Fig. 5 with details of statistical analysis), PNN intensity across the layers was significantly lower in the *Fmr1* KO than WT mice under all three experimental conditions. While PV intensity in this region was not different between *Fmr1* KO and WT mice in the control group, both Naïve and FC WT mice showed an increase in PV intensity compared to control WT, which was not observed in the *Fmr1* KO mice. In the amygdala (Sup. Fig. 6), both PV and PNN intensities were lower in the *Fmr1* KO mice under all experimental conditions compared to WT mice. In the DG of the hippocampus (Sup. Fig. 7), PNN intensity increased in WT mice after FC, but not in the *Fmr1* KO mice. In the CA1 region (Sup. Fig. 7), both Naïve and FC *Fmr1* KO mice showed an increase in PV intensity compared to control *Fmr1* KO mice, which was not observed in WT mice. This was reversed in the CA3 region (Sup. Fig. 8), where a significant increase in PV intensity was seen in both Naïve and FC WT compared to controls, but not *Fmr1* KO mice. The CA2 region of the hippocampus showed increased PNN intensity following FC in WT and *Fmr1* KO mice, but PNN intensity remained significantly lower in *Fmr1* KO compared to WT mice. Taken together, this additional analysis supports the notion that impaired PV and PNN expression in Fmr1 KO mice and/or alterations in their dynamics following learning, may contribute to learning deficits.

4. Discussion

In this study, we sought to determine whether CNS circuitry involved in fear-memory formation is altered in the *Fmr1* KO mice, focusing on PV interneurons and PNNs. Our data show a consistent impairment in tone-associated fear memory in *Fmr1* KO mice. Baseline PNN expression is reduced in the amygdala, auditory cortex and CA2 of *Fmr1* KO mice and PV expression is increased in the dentate gyrus. Fear conditioning causes a reduction in PV cell density in the auditory cortex across both genotypes and a differential regulation of PV in CA3 between WT and *Fmr1* KO mice. The density of PV cells in A1 that were surrounded by PNN did not change with conditioning. However, density of PV cells that were not surrounded by PNNs decreased following fear conditioning, suggesting these cells are more susceptible to learning induced plasticity. There was a positive correlation between overall density of PNNs and memory recall, in particular with tone recall, indicating that the lower levels of PNN found in amygdala and auditory cortex may underlie impaired tone-associated fear memories in *Fmr1* KO mice. These data provide a number of novel insights into memory deficits in FXS, suggesting in particular that PNNs may be the most relevant cellular structure predictive of deficient fear-memory association, consistent with findings of Banerjee et al. (2017).

4.1. Behavioral performance in Fmr1 KO mice and relationship to FXS

We found impaired tone-associated fear memory in *Fmr1* KO mice. Our data are consistent with the majority of studies in *Fmr1* KO mice on the FVB background that show deficits in fear conditioning (de Diego-Otero et al., 2009; Oddi et al., 2015; Olmos-Serrano et al., 2011; Romero-Zerbo et al., 2009; but see Dobkin et al., 2000). Reduced freezing after fear conditioning parallels human studies that found reduced activation of the amygdala in people with FXS in response to fearful stimuli such as fearful faces (Hessl et al., 2007, 2011; Kim et al., 2014). The reduced activation correlated with higher levels of anxiety (Kim et al., 2014) and with *Fmr1* gene expression. Interestingly, studies of anxiety disorders outside of the FXS population instead have found that people with anxiety disorders tend to have increased amygdala activation (reviewed in Shin & Liberzon, 2010), and potentiation of fear responses (Duits et al., 2015; Lissek et al., 2005). If it is generally true that people with anxiety have hyperactivation of amygdala while people with FXS tend to have hypo-activation, it's possible that mechanisms, which drive anxiety, are fundamentally different in FXS. It has been suggested that amygdala hyper-activation in people with anxiety may be due to an exaggerated response to a learned event or a persistent memory (Duits et al., 2015); instead the *Fmr1* KO mice, and potentially people with FXS, may have a reduced ability to properly associate a fearful stimulus. This remains to be explicitly tested. Future studies on anxiety using the *Fmr1* KO mouse might benefit from including other physiologic measures to correlate with behavioral anxiety tests.

In addition to freezing, we classified and scored other behaviors (Coimbra et al., 2017; Cruz et al., 1994; Rodgers & Johnson, 1995) to determine whether *Fmr1* KO mice displayed an alternate anxiety-related behavior in place of complete immobility. We found that *Fmr1* KO mice display a similar range of behaviors as WT mice, but they do not modify them to the extent that WT mice do after fear conditioning. In *Fmr1* KO mice, the observed changes were always attenuated compared to WT mice. It is unclear if such attenuated behavioral expression of fear learning is specific to the fear-conditioning task. The *Fmr1* KO mice show deficits in spatial memory, procedural memory and trace conditioning tasks as well (Baker et al., 2010; Vinueza Veloz et al., 2012; Zhao et al., 2005) and may show broad learning and memory deficits as also implied by the hippocampal synaptic deficits (Huber, Gallagher, Warren, & Bear, 2002). Additionally, WT mice change their behavior profile when the tone is played in the training context, preferring freezing to all other behaviors when environmental cues are the most predicative of shock. However, this was not observed in *Fmr1* KO mice. The behavior "scanning" as defined here is consistent with the "orienting" or "risk assessment" (reviewed in: Blanchard et al., 2011; Roelofs, 2017). Risk assessment behaviors such as "scanning/orienting" are thought to occur after a potential threat is detected. They help an animal choose the best defensive behavior for survival, including flight if there is an escape route, hiding if there is shelter, or freezing if neither flight nor hiding is possible. When both the tone and contextual cues were present WT mice switch from risk assessment behaviors to the defensive behavior of freezing, while the *Fmr1* KO mice do not show this shift in behavior. This is consistent with reports of behavioral inflexibility in FXS and autism (Amodeo, Jones, Sweeney, & Ragozzino, 2012; reviewed in Santos, Kanellopoulos, & Bagni, 2014).

4.2. PNN density in FXS

Both auditory cortex and amygdala play a role in the acquisition and/or consolidation of memory in fear conditioning paradigms. Here

we present novel data that both of these regions have reduced PNN density in adult *Fmr1* KO mice compared to WT mice, consistent with their impaired tone-associated memory. In the auditory cortex, intact PNNs are necessary for the consolidation of auditory fear conditioning (Banerjee et al., 2017). In the visual cortex, PNNs are implicated in consolidation of remote fear conditioned memories using visual cues (Thompson et al., 2018). Likewise PNNs in the amygdala have been shown to "protect" an established memory from erasure after the fear memory has undergone an extinction protocol (Gogolla et al., 2009). Whether abnormal basal levels of PNN in *Fmr1* KO mice contribute to reduced plasticity in the lateral amygdala (Zhao et al., 2005) that may underlie the fear memory deficits in these mice remain unclear. Our data show that the PNN levels change in the amygdala of both genotypes during both naïve and fear conditioning suggesting that PNN plasticity is not fear memory specific. However, the reduced basal PNN density in both amygdala regions examined was correlated with impaired freezing during the tone memory recall, whereas PV density showed no correlation with behavioral performance. This suggests that restoration of basal PNN density may be a promising target for improving behavioral performance in FXS.

There is a growing body of work suggesting a role for matrix metalloproteinase-9 (MMP-9) in FXS symptoms (reviewed in Reinhard, Razak, & Ethell, 2015). MMP-9 is an enzyme, which is elevated in FXS, and which may break down PNNs by cleaving ECM components. Genetically reducing MMP-9 levels in *Fmr1* KO mice using heterozygous MMP-9 KO mice crossed with *Fmr1* KO mice rescues PNN formation in the developing auditory cortex of *Fmr1* KO mice (Wen, Afroz, et al., 2018). To confirm whether reduced PNN levels in adult *Fmr1* KO mice have a causal role in impaired fear memory consolidation, future studies could pharmacologically inhibit MMP-9 in *Fmr1* KO mice during fear memory consolidation using a specific MMP-9 inhibitor. As PNNs are implicated in stabilizing neuronal circuits involved in memory consolidation (Banerjee et al., 2017; Gogolla et al., 2009; Happel et al., 2014; Hylin et al., 2013; Xue et al., 2014), our data suggest that reduced number of cells containing PNNs observed in both auditory cortex and amygdala of *Fmr1* KO mice may underlie impaired memory consolidation in *Fmr1* KO mice.

4.3. Modification of AC in fear conditioning and FXS

PNN density, specifically in the superficial layers of AC, decreased in WT mice after fear conditioning. Such plasticity in PNN density was not seen in *Fmr1* KO mice. Modification of superficial layers in WT mice is consistent with the known modification of circuitry in the auditory cortex in response to fear conditioning, where cholinergic input activates intracortical inhibition of layer 2/3 PV cells to disinhibit pyramidal cells (Letzkus et al., 2011) causing a shift in their receptive fields for better representation of the conditioning tone (Froemke et al., 2007). Our data suggest that PNN plasticity in the superficial layers of AC may be involved in this circuit modification process after fear conditioning.

There is a large body of work that identifies impaired PV cell function and/or expression in *Fmr1* KO mice across many brain regions and developmental stages (Gibson, Bartley, Hays, & Huber, 2008; Goel et al., 2018; Martin, Corbin, & Huntsman, 2014; Olmos-Serrano et al., 2010; Patel, Hays, Bureau, Huber, & Gibson, 2013; Selby, Zhang, & Sun, 2007; Wen, Afroz, et al., 2018). Therefore, we predicted impaired modification and/or impaired expression of PV in interneurons of *Fmr1* KO mice associated with fear conditioning. Our data show the novel finding that fear conditioning was associated with reduced number of cells expressing PV in the auditory cortex, particularly PV cells without PNN, but this modification was observed in both WT and *Fmr1* KO mice. The reduction in PV cell density in the auditory cortex is consistent with the previously reported cholinergic-induced disinhibition of cortical microcircuits, wherein PV cells are inhibited in the auditory cortex after fear conditioning to allow for potentiation of responses to the conditioning tone stimulus (Letzkus et al., 2011). PV cells slowly regain perisomal inhibition onto excitatory cells within a 2 h time frame after stimulation (Froemke et al., 2007). The reduction in PV cell density observed in this study is likely a reflection of reduced PV protein within inhibitory cells (Filice et al., 2016) in response to their sustained inhibition, making them less detectable with fluorescence imaging after IHC. The parameters involved in regulating PV protein expression after a change in network excitation/inhibition have not been determined, but it is clear that PV cells and/or PV protein expression are modulated in response to fear conditioning and environmental enrichment in the hippocampus (Donato et al., 2013) and after developmental manipulations in the auditory cortex (de Villers-Sidani, Chang, Bao, & Merzenich, 2007) and the visual cortex (Tropea et al., 2006). Intracellular signaling pathways within PV cells are activated within only 20 min of sound stimulation (Cohen et al., 2016). In the present study we observed reduced PV levels in both WT and *Fmr1* KO mice suggesting these changes are less likely to contribute to reduced tone-associated memory observed in *Fmr1* KO mice.

4.4. The hippocampal circuit

4.4.1. PV changes in DG and CA3

The role of inhibition is important for the flow of information within the hippocampus. Information typically flows from the entorhinal cortex (EC) into the dentate gyrus granule cells, with some projections from EC also innervating CA3 and CA2 (reviewed in Jones & McHugh, 2011). The DG is thought to be involved in pattern separation, in part due to the small population of cells activated by EC input which form non-overlapping populations for memory encoding. If inhibition is either largely increased or decreased in DG there is impaired spatial learning, indicating that if too many or too few DG granule cells are active, there is improper encoding of discrete contexts. Strong inhibition within the DG is thought to limit the population of activated of granule cells, thereby controlling the memory trace (reviewed in Fournier & Duman, 2013). In support of this, there is indeed strong activation of inhibition during novel context exploration (Nitz & McNaughton, 2004). From the DG, mossy fiber terminals innervate both excitatory and inhibitory cells in CA3, but contact a larger percentage of inhibitory cells (Acsady, Kamondi, Sık, Freund, & Buzsáki, 1998). This again suggests strong regional inhibition controls the population of cells coding for a memory in CA3.

In this study we observed an attenuated shift in behaviors in *Fmr1* KO mice during contextual recall. Although it did not result in significantly impaired total freezing, *Fmr1* KO mice showed reduced anxiety-like behaviors such as scanning during contextual recall. This reduction of response to the context was accompanied by modest changes in PV expression in DG and CA3 hippocampus in *Fmr1* KO mice and differential regulation of PNNs between WT and *Fmr1* KO mice.

Beginning with the region of input into the hippocampus, we found increased PV density in the DG of *Fmr1* KO mice. This was particularly pronounced after naïve or fear conditioning. This adds to a body of work indicating impaired function and morphology in the DG of FXS mice (reviewed in Bostrom et al., 2016; Ivanco & Greenough, 2002; Zhang et al., 2017). DG is known to respond to novel contexts (Davis, 2004; Moser, 1996) and also plays a role in pattern completion (reviewed in Knierim, 2015), spatial learning and memory (Andrews-Zwilling et al., 2012). The enhanced PV expression in DG of *Fmr1* KO mice may also explain impaired up-regulation of PV in CA3 of *Fmr1* KO mice following contextual learning due to a lower excitatory input from DG to CA3 inhibitory neurons.

There were observable changes to PV density in response to fear conditioning in the CA3 region of the hippocampus in WT but not in *Fmr1* KO mice. The increased PV density in WT mice is consistent with a previous report, which demonstrates increased intensity of PV expression after fear conditioning in CA3 (Donato et al., 2013). Activation of PV cells controlled performance on a hippocampal dependent memory

task and demonstrated that levels of PV in the CA3 relate to behavioral performance (Donato et al., 2013). However, environmental enrichment reduced PV intensity (Donato et al., 2013), which might be at odds with the increase in PV density in our naïve conditioned mice.

4.4.2. CA2 and PNNs

Information flows next from CA3 through CA2 and into CA1. CA2 is beginning to be recognized as having an important role in hippocampal-dependent memory, and in our data we observed that both PNN intensity and PV density were modulated in response to naïve or fear conditioning. CA2 synapses do not show long-term potentiation in response to Schaffer's collateral (CA3) stimulation, but instead CA3 mediates long-term depression of CA2 inhibitory cells synapsing onto CA2 excitatory cells (Nasrallah, Piskorowski, & Chevaleyre, 2015). In contrast to this disinhibitory effect of CA3 input into CA2, stimulation of Schaffer's collateral terminals (CA3 axons) causes reliable long-term potentiation in CA1. This highlights the important but variable role that inhibition plays within each region of the hippocampus.

We also observed reduced PNN levels under basal conditions in the CA2 of *Fmr1* KO mice. PNN structures within CA2 are thought to inhibit synaptic potentiation (Carstens et al., 2016), therefore reduced PNN intensity in *Fmr1* KO mice may suggest increased excitability in CA2 which would also be an interesting avenue for future studies. Neither CA2 nor DG showed modification of PV or PNNs specifically in response to fear conditioning.

4.4.3. PNN changes are dynamic

Although we did not observe modulation of PV or PNN in CA1 after fear conditioning in the tone-context experiment (30 min after contextual recall), significant changes were seen in the context-tone experiment 4 h after contextual recall. A similar phenomenon was observed in the DG of mice in the context-tone experiment. This differential modulation between experiments suggests that CA1 hippocampus is more dynamic in responding to alterations in the context, and possibly independent of the fear-associated component of the context. This is also consistent with a role for dorsal CA1 in context-specific memories and ventral CA1 in social and fear related memories (Fanselow & Dong, 2010). It has been noted that 'global remapping' of a context can take place in the hippocampus after changes to an environment (reviewed in Knierim, 2015) and observations presented here are consistent with CA1 and DG modifying their circuits in order to "update" the context memory after the animal has re-experienced the context without the shock. Strikingly changes in CA1 and DG 4 h after context re-exposure were quite similar: PV cell density was reduced in fear-conditioned mice, while modifications of PNNs in WT and *Fmr1* KO occurred in opposite directions (increased PNNs in WT and decreased PNNs in *Fmr1* KO mice). This again confirms the idea that PNN regulation is disrupted in *Fmr1* KO mice.

5. Conclusions

Taken together, we show a deficit in tone-shock associative learning in the *Fmr1* KO mouse, an animal model for FXS. Behavioral analysis involved not just the standard freeze-frame method, but also quantified additional mouse behaviors to rule out potential confounds of hyperactivity. Reduced baseline density and dynamics of PNN in the auditory cortex and amygdala may underlie impaired learning in the *Fmr1* KO mouse. The role of MMP-9 in the cleavage of PNN components, and the fact that MMP-9 is a target of FMRP translation control suggests the hypothesis that MMP-9 reduction either genetically, or with specific inhibitors, will normalize PNNs and fear conditioning in *Fmr1* KO mice. Future studies are needed to test this hypothesis.

6. Funding and disclosure

The authors declare no conflict of interest. This work was supported by the National Institute of Child Health and Human Development and the National Institute of Mental Health (1U54 HD082008-01 to I.M.E., D.K.B., and K.A.R.); U.S. Army Medical Research and Materiel Command (W81XWH-15-1-0436 and W81XWH-15-1-0434 to I.M.E., D.K.B., and K.A.R.), National Institute of Mental Health (MH67121 to I.M.E) and the National Science Foundation (graduate student research fellowship to S.M.R.).

Declaration of Competing Interest

None.

Acknowledgements

We thank members of the Ethell, Binder and Razak laboratories for helpful discussions and David Carter for advice on confocal microscopy. The authors declare no competing financial interests.

Appendix A. Supplementary material

Supplementary data to this article can be found online at https://doi.org/10.1016/j.nlm.2019.107042.

References

Acsady, L., Kamondi, A., Sık, A., Freund, T., & Buzsáki, G. (1998). GABAergic cells are the major postsynaptic targets of mossy fibers in the rat hippocampus. *Journal of Neuroscience, 18*, 3386–3403.

Amodeo, D. A., Jones, J. H., Sweeney, J. A., & Ragozzino, M. E. (2012). Differences in BTBR T+ tf/J and C57BL/6J mice on probabilistic reversal learning and stereotyped behaviors. *Behavioural Brain Research, 227*, 64–72.

Anderson, L. A., Christianson, G. B., & Linden, J. F. (2009). Mouse auditory cortex differs from visual and somatosensory cortices in the laminar distribution of cytochrome oxidase and acetylcholinesterase. *Brain Research, 1252*, 130–142.

Andreatta, M., Glotzbach-Schoon, E., Mühlberger, A., Schulz, S. M., Wiemer, J., & Pauli, P. (2015). Initial and sustained brain responses to contextual conditioned anxiety in humans. *Cortex, 63*, 352–363.

Andrews-Zwilling, Y., Gillespie, A. K., Kravitz, A. V., Nelson, A. B., Devidze, N., Lo, I., ... Huang, Y. (2012). Hilar GABAergic interneuron activity controls spatial learning and memory retrieval. *PLoS ONE, 7*, e40555.

Antunes, R., & Moita, M. A. (2010). Discriminative auditory fear learning requires both tuned and nontuned auditory pathways to the amygdala. *Journal of Neuroscience, 30*, 9782–9787.

Baker, K. B., Wray, S. P., Ritter, R., Mason, S., Lanthorn, T. H., & Savelieva, K. V. (2010). Male and female Fmr1 knockout mice on C57 albino background exhibit spatial learning and memory impairments. *Genes, Brain and Behavior, 9*(6), 562–574.

Bakker, C. E., & Oostra, B. A. (2003). Understanding fragile X syndrome: Insights from animal models. *Cytogenetic and Genome Research, 100*, 111–123.

Balmer, T. S. (2016). Perineuronal nets enhance the excitability of fast-spiking neurons. *eNeuro, 3*.

Banerjee, S. B., Gutzeit, V. A., Baman, J., Aoued, H. S., Doshi, N. K., Liu, R. C., & Ressler, K. J. (2017). Perineuronal nets in the adult sensory cortex are necessary for fear learning. *Neuron, 95*, 169–179.e3.

Beurdeley, M., Spatazza, J., Lee, H. H., Sugiyama, S., Bernard, C., Di Nardo, A. A., ... Prochiantz, A. (2012). Otx2 binding to perineuronal nets persistently regulates plasticity in the mature visual cortex. *Journal of Neuroscience, 32*, 9429–9437.

Blanchard, D. C., Griebel, G., Pobbe, R., & Blanchard, R. J. (2011). Risk assessment as an evolved threat detection and analysis process. *Neuroscience & Biobehavioral Reviews, 35*, 991–998.

Bostrom, C., Yau, S., Majaess, N., Vetrici, M., Gil-Mohapel, J., & Christie, B. R. (2016). Hippocampal dysfunction and cognitive impairment in Fragile-X Syndrome. *Neuroscience & Biobehavioral Reviews, 68*, 563–574.

Çalışkan, G., Müller, I., Semtner, M., Winkelmann, A., Raza, A. S., Hollnagel, J. O., ... Meier, J. C. (2016). Identification of parvalbumin interneurons as cellular substrate of fear memory persistence. *Cerebral Cortex, 26*, 2325–2340.

Carstens, K. E., Phillips, M. L., Pozzo-Miller, L., Weinberg, R. J., & Dudek, S. M. (2016). Perineuronal nets suppress plasticity of excitatory synapses on CA2 pyramidal neurons. *The Journal of Neuroscience, 36*, 6312–6320.

Castrén, M., Pääkkönen, A., Tarkka, I. M., Ryynänen, M., & Partanen, J. (2003). Augmentation of auditory N1 in children with fragile X syndrome. *Brain Topography, 15*, 165–171.

Cohen, S. M., Ma, H., Kuchibhotla, K. V., Watson, B. O., Buzsáki, G., Froemke, R. C., & Tsien, R. W. (2016). Excitation-transcription coupling in parvalbumin-positive interneurons employs a novel CaM Kinase-dependent pathway distinct from excitatory neurons. *Neuron, 90*, 292–307.

Coimbra, N. C., Paschoalin-Maurin, T., Bassi, G. S., Kanashiro, A., Biagioni, A. F., Felippotti, T. T., ... Lobão-Soares, B. (2017). Critical neuropsychobiological analysis of panic attack- and anticipatory anxiety-like behaviors in rodents confronted with snakes in polygonal arenas and complex labyrinths: A comparison to the elevated

plus- and T-maze behavioral tests. *Revista Brasileira de Psiquiatria, 39*, 72–83.
Cornish, K. M., Munir, F., & Cross, G. (2001). Differential impact of the FMR-1 full mutation on memory and attention functioning: A neuropsychological perspective. *Journal of Cognitive Neuroscience, 13*, 144–150.
Cruz, A. P. M., Frei, F., & Graeff, F. G. (1994). Ethnopharmacological analysis of rat behavior on the elevated plus-maze. *Pharmocology Biochemistry and Behavior, 49*, 171–176.
Daumas, S. (2005). Encoding, consolidation, and retrieval of contextual memory: Differential involvement of dorsal CA3 and CA1 hippocampal subregions. *Learning & Memory, 12*, 375–382.
Davis, C. D. (2004). Novel environments enhance the induction and maintenance of long-term potentiation in the dentate gyrus. *Journal of Neuroscience, 24*, 6497–6506.
de Diego-Otero, Y., Romero-Zerbo, Y., el Bekay, R., Decara, J., Sanchez, L., Rodriguez-de Fonseca, F., & del Arco-Herrera, I. (2009). α-tocopherol protects against oxidative stress in the fragile X knockout mouse: An experimental therapeutic approach for the Fmr1 deficiency. *Neuropsychopharmacology, 34*, 1011.
Dityatev, A., Brückner, G., Dityateva, G., Grosche, J., Kleene, R., & Schachner, M. (2007). Activity-dependent formation and functions of chondroitin sulfate-rich extracellular matrix of perineuronal nets. *Developmental Neurobiology, 67*, 570–588.
Dobkin, C., Rabe, A., Dumas, R., El Idrissi, A., Haubenstock, H., & Brown, W. T. (2000). Fmr1 knockout mouse has a distinctive strain-specific learning impairment. *Neuroscience, 100*, 423–429.
Donato, F., Rompani, S. B., & Caroni, P. (2013). Parvalbumin-expressing basket-cell network plasticity induced by experience regulates adult learning. *Nature, 504*, 272–276.
Duits, P., Cath, D. C., Lissek, S., Hox, J. J., Hamm, A. O., Engelhard, I. M., ... Baas, J. M. P. (2015). Updated meta-analysis of classical fear conditioning in the anxiety disorders. *Depression and Anxiety, 32*, 239–253.
Dziembowska, M., Pretto, D. I., Janusz, A., Kaczmarek, L., Leigh, M. J., Gabriel, N., ... Tassone, F. (2013). High MMP-9 activity levels in fragile X syndrome are lowered by minocycline. *American Journal of Medical Genetics Part A, 161*, 1897–1903.
Eadie, B. D., Cushman, J., Kannangara, T. S., Fanselow, M. S., & Christie, B. R. (2012). NMDA receptor hypofunction in the dentate gyrus and impaired context discrimination in adult Fmr1 knockout mice. *Hippocampus, 22*, 241–254.
Esclassan, F., Coutureau, E., Di Scala, G., & Marchand, A. R. (2009). Differential contribution of dorsal and ventral hippocampus to trace and delay fear conditioning. *Hippocampus, 19*, 33–44.
Fanselow, M. S., & Dong, H.-W. (2010). Are the dorsal and ventral hippocampus functionally distinct structures? *Neuron, 65*, 7–19.
Favuzzi, E., Marques-Smith, A., Deogracias, R., Winterflood, C. M., Sánchez-Aguilera, A., Mantoan, L., ... Rico, B. (2017). Activity-dependent gating of parvalbumin interneuron function by the perineuronal net protein brevican. *Neuron, 95*, 639–655.e10.
Filice, F., Vörckel, K. J., Sungur, A.Ö., Wöhr, M., & Schwaller, B. (2016). Reduction in parvalbumin expression not loss of the parvalbumin-expressing GABA interneuron subpopulation in genetic parvalbumin and shank mouse models of autism. Molecular. *Brain, 9*.
Fournier, N. M., & Duman, R. S. (2013). Illuminating hippocampal control of fear memory and anxiety. *Neuron, 77*, 803–806.
Froemke, R. C., Merzenich, M. M., & Schreiner, C. E. (2007). A synaptic memory trace for cortical receptive field plasticity. *Nature, 450*, 425.
Gibson, J. R., Bartley, A. F., Hays, S. A., & Huber, K. M. (2008). Imbalance of neocortical excitation and inhibition and altered UP states reflect network hyperexcitability in the mouse model of fragile X syndrome. *Journal of Neurophysiology, 100*, 2615–2626.
Goel, A., Cantu, D. A., Guilfoyle, J., Chaudhari, G. R., Newadkar, A., Todisco, B., ... Erickson, C. A. (2018). Impaired perceptual learning in a mouse model of Fragile X syndrome is mediated by parvalbumin neuron dysfunction and is reversible. *Nature Neuroscience, 21*, 1404–1411.
Gogolla, N., Caroni, P., Lüthi, A., & Herry, C. (2009). Perineuronal nets protect fear memories from erasure. *Science, 325*, 1258–1261.
Hagerman, R. J., & Hagerman, P. J. (2002). The fragile X premutation: Into the phenotypic fold. *Current Opinion in Genetics & Development, 12*, 278–283.
Happel, M. F. K., Niekisch, H., Castiblanco Rivera, L. L., Ohl, F. W., Deliano, M., & Frischknecht, R. (2014). Enhanced cognitive flexibility in reversal learning induced by removal of the extracellular matrix in auditory cortex. *Proceedings of the National Academy of Sciences, 111*, 2800–2805.
Harkness, J. H., Bushana, P. N., Todd, R. P., Clegern, W. C., Sorg, B. A., & Wisor, J. P. (2018). Sleep disruption elevates oxidative stress in parvalbumin-positive cells of the rat cerebral cortex. *Sleep, 42*(1), zsy201.
Hessl, D., Rivera, S., Koldewyn, K., Cordeiro, L., Adams, J., Tassone, F., ... Hagerman, R. J. (2007). Amygdala dysfunction in men with the fragile X premutation. *Brain, 130*, 404–416.
Hessl, D., Wang, J. M., Schneider, A., Koldewyn, K., Le, L., Iwahashi, C., ... Rivera, S. M. (2011). Decreased fragile X mental retardation protein expression underlies amygdala dysfunction in carriers of the fragile X premutation. *Biological Psychiatry, 70*, 859–865.
Huber, K. M., Gallagher, S. M., Warren, S. T., & Bear, M. F. (2002). Altered synaptic plasticity in a mouse model of fragile X mental retardation. *Proceedings of the National Academy of Sciences, 99*, 7746–7750.
Hylin, M. J., Orsi, S. A., Moore, A. N., & Dash, P. K. (2013). Disruption of the perineuronal net in the hippocampus or medial prefrontal cortex impairs fear conditioning. *Learning & Memory, 20*, 267–273.
Ivanco, T. L., & Greenough, W. T. (2002). Altered mossy fiber distributions in adult Fmr1 (FVB) knockout mice. *Hippocampus, 12*, 47–54.
Jones, M. W., & McHugh, T. J. (2011). Updating hippocampal representations: CA2 joins the circuit. *Trends in Neurosciences, 34*, 526–535.
Kim, S.-Y., Burris, J., Bassal, F., Koldewyn, K., Chattarji, S., Tassone, F., ... Rivera, S. M. (2014). Fear-specific amygdala function in children and adolescents on the fragile X spectrum: A dosage response of the FMR1 gene. *Cerebral Cortex, 24*, 600–613.
Knierim, J. J. (2015). The hippocampus. *Current Biology, 25*, R1107–R1125.
Kooy, R. F., D'Hooge, R., Reyniers, E., Bakker, C. E., Nagels, G., De Boulle, K., ... Oostra, B. A. (1996). Transgenic mouse model for the fragile X syndrome. *American Journal of Medical Genetics, 64*, 241–245.
LaBar, K. S., Gatenby, J. C., Gore, J. C., LeDoux, J. E., & Phelps, E. A. (1998). Human amygdala activation during conditioned fear acquisition and extinction: A mixed-trial fMRI study. *Neuron, 20*, 937–945.
Lee, H., Leamey, C. A., & Sawatari, A. (2012). Perineuronal nets play a role in regulating striatal function in the mouse. *PLoS One, 7*, e32747.
Letzkus, J. J., Wolff, S. B. E., Meyer, E. M. M., Tovote, P., Courtin, J., Herry, C., & Lüthi, A. (2011). A disinhibitory microcircuit for associative fear learning in the auditory cortex. *Nature, 480*, 331–335.
Lissek, S., Powers, A. S., McClure, E. B., Phelps, E. A., Woldehawariat, G., Grillon, C., & Pine, D. S. (2005). Classical fear conditioning in the anxiety disorders: A meta-analysis. *Behavior Research and Therapy, 43*, 1391–1424.
Lovelace, J. W., Wen, T. H., Reinhard, S., Hsu, M. S., Sidhu, H., Ethell, I. M., ... Razak, K. A. (2016). Matrix metalloproteinase-9 deletion rescues auditory evoked potential habituation deficit in a mouse model of Fragile X Syndrome. *Neurobiology of Disease, 89*, 126–135.
Martin, B. S., Corbin, J. G., & Huntsman, M. M. (2014). Deficient tonic GABAergic conductance and synaptic balance in the fragile X syndrome amygdala. *Journal of Neurophysiology, 112*, 890–902.
McRae, P. A., Rocco, M. M., Kelly, G., Brumberg, J. C., & Matthews, R. T. (2007). Sensory deprivation alters aggrecan and perineuronal net expression in the mouse barrel cortex. *Journal of Neuroscience, 27*, 5405–5413.
Miller, L. J., McIntosh, D. N., McGrath, J., Shyu, V., Lampe, M., Taylor, A. K., ... Hagerman, R. J. (1999). Electrodermal responses to sensory stimuli in individuals with fragile X syndrome: A preliminary report. *American Journal of Medical Genetics, 83*, 268–279.
Morrison, D. J., Rashid, A. J., Yiu, A. P., Yan, C., Frankland, P. W., & Josselyn, S. A. (2016). Parvalbumin interneurons constrain the size of the lateral amygdala engram. *Neurobiology of Learning and Memory, 135*, 91–99.
Moser, E. I. (1996). Altered inhibition of dentate granule cells during spatial learning in an exploration task. *Journal of Neuroscience, 16*, 1247–1259.
Nasrallah, K., Piskorowski, R. A., & Chevaleyre, V. (2015). Inhibitory plasticity permits the recruitment of CA2 pyramidal neurons by CA3. *eNeuro, 2*.
Nitz, D., & McNaughton, B. (2004). Differential modulation of CA1 and dentate gyrus interneurons during exploration of novel environments. *Journal of Neurophysiology, 91*, 863–872.
Oddi, D., Subashi, E., Middei, S., Bellocchio, L., Lemaire-Mayo, V., Guzmán, M., ... Pietropaolo, S. (2015). Early social enrichment rescues adult behavioral and brain abnormalities in a mouse model of fragile X syndrome. *Neuropsychopharmacology, 40*, 1113.
Ognjanovski, N., Schaeffer, S., Wu, J., Mofakham, S., Maruyama, D., Zochowski, M., & Aton, S. J. (2017). Parvalbumin-expressing interneurons coordinate hippocampal network dynamics required for memory consolidation. *Nature Communications, 8*, 15039.
Olmos-Serrano, J. L., Corbin, J. G., & Burns, M. P. (2011). The $GABA_A$ receptor agonist THIP ameliorates specific behavioral deficits in the mouse model of fragile X syndrome. *Developmental Neuroscience, 33*, 395–403.
Olmos-Serrano, J. L., Paluszkiewicz, S. M., Martin, B. S., Kaufmann, W. E., Corbin, J. G., & Huntsman, M. M. (2010). Defective GABAergic neurotransmission and pharmacological rescue of neuronal hyperexcitability in the amygdala in a mouse model of fragile X syndrome. *Journal of Neuroscience, 30*, 9929–9938.
Paradee, W., Melikian, H. E., Rasmussen, D. L., Kenneson, A., Conn, P. J., & Warren, S. T. (1999). Fragile X mouse: Strain effects of knockout phenotype and evidence suggesting deficient amygdala function. *Neuroscience, 94*, 185–192.
Patel, A. B., Hays, S. A., Bureau, I., Huber, K. M., & Gibson, J. R. (2013). A target cell-specific role for presynaptic Fmr1 in regulating glutamate release onto neocortical fast-spiking inhibitory neurons. *Journal of Neuroscience, 33*, 2593–2604.
Phillips, R. G., & LeDoux, J. E. (1992). Differential contribution of amygdala and hippocampus to cued and contextual fear conditioning. *Behavioral Neuroscience, 106*, 274.
Pizzorusso, T., Medini, P., Berardi, N., Chierzi, S., Fawcett, J. W., & Maffei, L. (2002). Reactivation of ocular dominance plasticity in the adult visual cortex. *Science, 298*, 1248–1251.
Quirk, G. J., Armony, J. L., & LeDoux, J. E. (1997). Fear conditioning enhances different temporal components of tone-evoked spike trains in auditory cortex and lateral amygdala. *Neuron, 19*, 613–624.
Reinhard, S. M., Razak, K., & Ethell, I. M. (2015). A delicate balance: Role of MMP-9 in brain development and pathophysiology of neurodevelopmental disorders. *Frontiers in Cellular Neuroscience, 9*.
Rodgers, R. J., & Johnson, N. J. T. (1995). Factor analysis of spatiotemporal and ethological measures in the murine elevated plus-maze test of anxiety. *Pharmocology Biochemistry and Behavior, 52*, 297–303.
Roelofs, K. (2017). Freeze for action: Neurobiological mechanisms in animal and human freezing. *Philosophical Transactions of the Royal Society B: Biological Sciences, 372*, 20160206.
Romero-Zerbo, Y., Decara, J., el Bekay, R., Sanchez-Salido, L., Del Arco-Herrera, I., de Fonseca, F. R., & de Diego-Otero, Y. (2009). Protective effects of melatonin against oxidative stress in Fmr1 knockout mice: A therapeutic research model for the fragile X syndrome. *Journal of Pineal Research, 46*, 224–234.
Roy, D. S., Kitamura, T., Okuyama, T., Ogawa, S. K., Sun, C., Obata, Y., ... Tonegawa, S. (2017). Distinct neural circuits for the formation and retrieval of episodic memories.

Cell, 170, 1000–1012.e19.
Santoro, M. R., Bray, S. M., & Warren, S. T. (2012). Molecular mechanisms of fragile X syndrome: A twenty-year perspective. *Annual Review of Pathology: Mechanisms of Disease, 7*, 219–245.
Santos, A. R., Kanellopoulos, A. K., & Bagni, C. (2014). Learning and behavioral deficits associated with the absence of the fragile X mental retardation protein: what a fly and mouse model can teach us. *Learning & Memory, 21*, 543–555.
Selby, L., Zhang, C., & Sun, Q.-Q. (2007). Major defects in neocortical GABAergic inhibitory circuits in mice lacking the fragile X mental retardation protein. *Neuroscience Letters, 412*, 227–232.
Shin, L. M., & Liberzon, I. (2010). The neurocircuitry of fear, stress, and anxiety disorders. *Neuropsychopharmacology, 35*, 169–191.
Sidhu, H., Dansie, L. E., Hickmott, P. W., Ethell, D. W., & Ethell, I. M. (2014). Genetic removal of matrix metalloproteinase 9 rescues the symptoms of fragile X syndrome in a mouse model. *Journal of Neuroscience, 34*, 9867–9879.
Slaker, M., Barnes, J., Sorg, B. A., & Grimm, J. W. (2016a). Impact of environmental enrichment on perineuronal nets in the prefrontal cortex following early and late abstinence from sucrose self-administration in rats. *PloS one, 11*(12), e0168256.
Slaker, M., Blacktop, J. M., & Sorg, B. A. (2016b). Caught in the net: Perineuronal nets and addiction. *Neural Plasticity, 2016*.
Slaker, M., Churchill, L., Todd, R. P., Blacktop, J. M., Zuloaga, D. G., Raber, J., Darling, R. A., Brown, T. E., & Sorg, B. A. (2015). Removal of perineuronal nets in the medial prefrontal cortex impairs the acquisition and reconsolidation of a cocaine-induced conditioned place preference memory. *Journal of Neuroscience, 35*, 4190–4202.
Slaker, M. L., Harkness, J. H., & Sorg, B. A. (2016). A standardized and automated method of perineuronal net analysis using Wisteria floribunda agglutinin staining intensity. *IBRO Reports, 1*, 54–60.
Sullivan, K., Hooper, S., & Hatton, D. (2007). Behavioral equivalents of anxiety in children with fragile X syndrome: Parent and teacher report. *Journal of Intellectual Disability Research, 51*, 54–65.
Takesian, A. E., & Hensch, T. K. (2013). Balancing plasticity/stability across brain development. *Progress in Brain Research, 207*, 3–34.
Tellez, A., Garcia, C. H., & Corral-Verdugo, V. (2015). Effect size, confidence intervals and statistical power in psychological research. *Psychology in Russia: State of the Art, 8*, 27–46.
Thomas, A. M., Bui, N., Graham, D., Perkins, J. R., Yuva-Paylor, L. A., & Paylor, R. (2011). Genetic reduction of group 1 metabotropic glutamate receptors alters select behaviors in a mouse model for fragile X syndrome. *Behavioural Brain Research, 223*, 310–321.
Thompson, E. H., Lensjø, K. K., Wigestrand, M. B., Malthe-Sørenssen, A., Hafting, T., & Fyhn, M. (2018). Removal of perineuronal nets disrupts recall of a remote fear memory. *Proceedings of the National Academy of Sciences, 115*, 607–612.
Tropea, D., Kreiman, G., Lyckman, A., Mukherjee, S., Yu, H., Horng, S., & Sur, M. (2006). Gene expression changes and molecular pathways mediating activity-dependent plasticity in visual cortex. *Nature Neuroscience, 9*, 660–668.
Ueno, H., Takao, K., Suemitsu, S., Murakami, S., Kitamura, N., Wani, K., ... Ishihara, T. (2018). Age-dependent and region-specific alteration of parvalbumin neurons and perineuronal nets in the mouse cerebral cortex. *Neurochemistry International, 112*, 59–70.
de Villers-Sidani, E., Chang, E. F., Bao, S., & Merzenich, M. M. (2007). Critical period window for spectral tuning defined in the primary auditory cortex (A1) in the rat. *Journal of Neuroscience, 27*, 180–189.
Vinueza Veloz, M. F., Buijsen, R. A. M., Willemsen, R., Cupido, A., Bosman, L. W., Koekkoek, S. K., ... De Zeeuw, C. I. (2012). The effect of an mGluR5 inhibitor on procedural memory and avoidance discrimination impairments in Fmr1 KO mice. *Genes, Brain and Behavior, 11*, 325–331.
Wen, T. H., Afroz, S., Reinhard, S. M., Palacios, A. R., Tapia, K., Binder, D. K., ... Ethell, I. M. (2018). Genetic reduction of matrix metalloproteinase-9 promotes formation of perineuronal nets around parvalbumin-expressing interneurons and normalizes auditory cortex responses in developing Fmr1 knock-out mice. *Cerebral Cortex, 28*, 3951–3964.
Wen, T. H., Binder, D. K., Ethell, I. M., & Razak, K. A. (2018). The perineuronal 'safety' net? Perineuronal net abnormalities in neurological disorders. *Frontiers in Molecular Neuroscience, 11*.
Xue, Y.-X., Xue, L.-F., Liu, J.-F., He, J., Deng, J.-H., Sun, S.-C., ... Lu, L. (2014). Depletion of perineuronal nets in the amygdala to enhance the erasure of drug memories. *Journal of Neuroscience, 34*, 6647–6658.
Yoo, H. (2015). Genetics of autism spectrum disorder: Current status and possible clinical applications. *Experimental Neurobiology, 24*, 257.
Zhang, N., Peng, Z., Tong, X., Lindemeyer, A. K., Cetina, Y., Huang, C. S., ... Houser, C. R. (2017). Decreased surface expression of the δ subunit of the GABA-A receptor contributes to reduced tonic inhibition in dentate granule cells in a mouse model of fragile X syndrome. *Experimental Neurology, 297*, 168–178.
Zhao, M. G., Toyoda, H., Ko, S. W., Ding, H. K., Wu, L. J., & Zhuo, M. (2005). Deficits in trace fear memory and long-term potentiation in a mouse model for fragile X syndrome. *Journal of Neuroscience, 25*, 7385–7392.